

Multivariate Overnight GARCH-Itô Model with Applications in Large Volatility Matrix Estimation and Prediction

Donggyu Kim¹, Minseog Oh¹, Xinyu Song², and Yazhen Wang³

¹College of Business,

Korea Advanced Institute of Science and Technology

²School of Statistics and Management,

Shanghai University of Finance and Economics

³Department of Statistics,

University of Wisconsin-Madison

April 15, 2022

Abstract

This paper introduces a unified multivariate overnight GARCH-Itô model for volatility matrix estimation and prediction both in the low- and high-dimensional set-up. To account for whole-day market dynamics in the financial market, the proposed model has two different instantaneous volatility processes for the open-to-close and close-to-open periods, while each embeds the discrete-time multivariate GARCH model structure. We call it the multivariate overnight GARCH-Itô (MOGI) model. Based on the connection between the discrete-time model structure and the continuous-time diffusion process, we propose a weighted least squares estimation procedure for estimating model parameters with open-to-close high-frequency and close-to-open low-frequency financial data, and establish its asymptotic theorems. We further discuss the prediction of future vast volatility matrices and study its asymptotic properties. A simulation study is conducted to check the finite sample performance of the proposed estimation and prediction methods. The empirical analysis is carried out to compare the performance

of the proposed MOGI model with other benchmark methods in portfolio allocation problems.

Keywords: Factor model, high dimensionality, low-rank, POET, quasi-maximum likelihood estimation, realized volatility matrix estimator, sparsity, overnight risk

1 Introduction

Volatility estimation and prediction are vibrant research areas in financial econometrics and statistics. There exist two major streams for studying volatility processes. The traditional stream adopts discrete-time parametric econometric models and employs low-frequency observations such as daily, weekly, or monthly asset returns. The discrete-time models employ GARCH structures to explain the dynamic evolution of the volatility process and are easy to implement in financial applications. The well-known models include the ARCH (Engle, 1982) and the GARCH models (Bollerslev, 1986) for the univariate case, and the VEC-GARCH (Bollerslev et al., 1988), the BEKK (Engle and Kroner, 1995), the CCC-GARCH (Bollerslev, 1990), and the DCC-GARCH models (Engle, 2002) for the multivariate case. On the other hand, the rather modern stream is constructed based on the continuous-time diffusion process and employs high-frequency observations, such as transaction-by-transaction stock prices. Given high-frequency data, nonparametric realized volatility estimators are constructed to estimate integrated volatilities. Examples of such estimators include the following: two-time scale realized volatility (Zhang et al., 2005), multi-scale realized volatility (Zhang, 2006, 2011), wavelet estimator (Fan and Wang, 2007), kernel realized volatility (Barndorff-Nielsen et al., 2008, 2011), pre-averaging realized volatility (Christensen et al., 2010; Jacod et al., 2009), quasi-maximum likelihood estimator (Aït-Sahalia et al., 2010; Xiu, 2010), local method of moments (Bibinger et al., 2014), and robust pre-averaging realized volatility (Fan and Kim, 2018). The above estimators exist both in the univariate and multivariate forms, and can estimate historical volatility well, but, lack the structure to describe the rich dynamics in the volatility process. This motivates us to develop dynamic models for the high-frequency data that embeds the discrete-time model structures.

Although researchers in the past followed the two streams rather independently, there have been some recent attempts to bridge the gaps between the discrete-time models and the continuous-time diffusion process for volatility analysis. Examples include Engle and Gallo (2006); Hansen et al. (2012); Shephard and Sheppard (2010); Tao et al. (2011). Recently, for a single asset, Kim and Wang (2016) introduced the unified GARCH-Itô model that embeds the univariate GARCH model structure in the continuous Itô diffusion process. The unified GARCH-Itô model employs the GARCH model structure to explain volatility evolution and to make inference on model parameters with combined high-frequency and low-frequency data. As a result, their proposed estimation procedure for GARCH model parameters provides more accurate results, and the GARCH structure provides a method to predict future daily integrated volatility with its conditional expectation. See also Song et al. (2021). However, these parametric models face the non-availability problem of high-frequency financial data during the market close-to-open period. Thus, they are usually developed only based on the open-to-close period, which results in underestimated market risk. To account for the whole-day market dynamics, Kim and Wang (2021) introduced the overnight GARCH-Itô model, which has two different instantaneous volatility processes for the open-to-close and close-to-open periods, respectively. Empirical studies have supported incorporation of the close-to-open periods for explaining the whole-day market dynamics (Kim and Wang, 2021). Recently, to analyze the risk contagion between the U.S. and China stock markets, Oh and Kim (2021) proposed the overnight diffusion process, which can accommodate the fact that volatility transmission occurs through overnight volatility processes. In financial applications, we are often required to explore the dynamics of the correlations among assets, which leads us to extend the univariate overnight GARCH-Itô model to a multivariate form.

In this paper, we propose the multivariate overnight GARCH-Itô (MOGI) model. When the number of assets is finite, the proposed model embeds the discrete-time multivariate GARCH model structure within its instantaneous volatility process. For example, the instantaneous volatility process of the MOGI model is obtained by some quadratic interpolation of the BEKK(1,1) model introduced by Engle and Kroner (1995). Specifically, for the open-

to-close period, the instantaneous volatility process has the current integrated volatility as an innovation, whereas for the close-to-open period, the instantaneous volatility process has the current squared log returns as an innovation. The conditional integrated volatility is expressed as a function of historical open-to-close integrated volatility matrices and squared close-to-open log returns. To make inferences for the parameters of the MOGI model, we introduce a weighted least squares estimation procedure that assigns different weights to the open-to-close and close-to-open volatilities. Specifically, we obtain the realized volatility matrix estimator based on open-to-close high-frequency data and use it as a proxy for the open-to-close conditional integrated volatility, whereas we use squared close-to-open returns as a proxy for the close-to-open conditional integrated volatility. These proxies have heterogeneous covariances that are related to the accuracy of the proxies. That is, we assume that the close-to-open and open-to-close volatilities have different dynamic structures. To reflect this, we first estimate sample covariances for the close-to-open and open-to-close proxies, and then assign different weights based on the sample covariances to evaluate the proposed weighted squares loss function. Finally, we discuss the consistency and asymptotic normality of the proposed estimation procedure.

In financial practices, we often encounter a large number of assets in portfolio allocation and risk management problems. In this paper, we also propose a large volatility matrix estimation and prediction procedure based on the high-dimensional factor Itô diffusion process. This approximate factor model decomposes the large volatility matrix into the latent factor volatility matrix that has low-rank, and the idiosyncratic volatility matrix that is sparse. Based on the approximate factor model, Kim and Fan (2019) introduced the factor GARCH-Itô model that describes the eigenvalue process of the latent factor volatility matrix by a unified GARCH-Itô model structure (Kim and Wang, 2016). In this paper, we further generalize this structure by embedding the discrete-time multivariate GARCH model structure in the latent factor volatility process. Under this high-dimensional set-up, we encounter an additional step of identifying and estimating the latent factor loading and factor volatility matrices. Given the proposed MOGI model structure, and under some conditions, the factor loading matrix can be estimated consistently with the eigenmatrix or the

group membership matrix (Aït-Sahalia and Xiu, 2017; Kim et al., 2018; Kim and Fan, 2019; Kim et al., 2020). The latent factor volatility matrices can be also identified and estimated consistently. Given the low-rank factor volatility matrix estimators, we follow the estimation procedure proposed in the low-dimensional case to obtain model parameter estimators. The proposed MOGI model structure allows us to estimate the future integrated factor volatility matrix. On the other hand, to account for the inherent sparse structure in the idiosyncratic volatility matrix, we employ the principal orthogonal component thresholding (POET) procedure introduced by Fan et al. (2013, 2016) to estimate the idiosyncratic volatility matrix. By combining the estimators for the future factor and idiosyncratic volatility matrices, we introduce an estimator for the conditional expectation of the future large volatility matrix. The asymptotic theorems for the proposed estimator are established.

The rest of the paper is organized as follows. Section 2 introduces the MOGI model and studies its properties. Section 3 develops the weighted least squares estimation procedure for model parameters and establishes its asymptotic theorems. Section 4 extends the MOGI model to the high-dimensional set-up and discusses how to harness the proposed model structure to estimate the future large volatility matrix. We present the asymptotic properties of the proposed estimator. In Section 5, we conduct a simulation study to validate the finite sample performance of the proposed estimation methods. Section 6 applies the MOGI model to empirical data. Proofs are collected in the Appendix.

2 Multivariate GARCH-Itô models

First, let us fix the notations. The operator \otimes denotes the Kronecker product, $\text{vec}(\cdot)$ denotes the operator that stacks the columns of a matrix, and $\text{vech}(\cdot)$ is a column vector obtained by vectorizing only the lower triangular part of a matrix. Moreover, $\text{vec}^{-1}(\cdot)$ denotes the inverse operator of $\text{vec}(\cdot)$. For any given p_1 -by- p_2 matrix $\mathbf{M} = (M_{ij})_{i=1,\dots,p_1,j=1,\dots,p_2}$, denote its matrix spectral norm by $\|\mathbf{M}\|_2$, its Frobenius norm by $\|\mathbf{M}\|_F = \sqrt{\text{Tr}(\mathbf{M}^\top \mathbf{M})}$, and $\|\mathbf{M}\|_{\max} = \max_{i,j} |M_{ij}|$. Let C be a generic constant whose values are free of $\boldsymbol{\theta}$, n , m , and p , and may change from occurrence to occurrence.

Let $\mathbf{X}(t) = (X_1(t), \dots, X_p(t))^\top$ be the vector of true underlying log prices of p assets at time t , which obeys the following continuous-time diffusion process:

$$d\mathbf{X}(t) = \boldsymbol{\mu}dt + \boldsymbol{\sigma}_t^\top d\mathbf{B}_t,$$

where $\boldsymbol{\mu} \in \mathbb{R}^p$ is a drift vector, $\boldsymbol{\sigma}_t$ is a p -by- p matrix, and \mathbf{B}_t is a p -dimensional standard Brownian motion. The stochastic process $\boldsymbol{\sigma}_t$ is defined on a filtered probability space $(\Omega, \mathcal{F}, \{\mathcal{F}_t, t \in [0, \infty)\}, P)$ with the filtration \mathcal{F}_t satisfying the usual conditions. The instantaneous (or spot) volatility process of $\mathbf{X}(t)$ is

$$\boldsymbol{\Sigma}_t = \boldsymbol{\sigma}_t^\top \boldsymbol{\sigma}_t$$

while the corresponding daily integrated volatility matrix of the n th day is

$$\boldsymbol{\Gamma}_n = \int_{n-1}^n \boldsymbol{\Sigma}_t dt = \int_{n-1}^{\tau+n-1} \boldsymbol{\Sigma}_t dt + \int_{\tau+n-1}^n \boldsymbol{\Sigma}_t dt,$$

where τ is the length of the open-to-close period. For a single asset, Kim and Wang (2021) introduced the overnight GARCH-Itô model that has two different instantaneous volatility processes for the open-to-close and close-to-open periods, respectively, and can accommodate both the discrete-time GARCH model structure and the continuous-time Itô diffusion process. During the open-to-close period, high-frequency data are observed so that volatility-related information can be reflected by the market price immediately, whereas during the close-to-open period, high-frequency data are not available and we usually cannot react to the overnight information immediately. To represent this, the overnight GARCH-Itô model used the open-to-close integrated volatility and the close-to-open squared log return as innovations. By embedding the GARCH structure and employing two types of innovations for modeling the instantaneous volatility process, the overnight GARCH-Itô model can explain the market dynamics very well. In this paper, we extend the univariate overnight GARCH-Itô model to the multivariate form. Specifically, we embed the well-known BEKK(1,1) model structure (Engle and Kroner, 1995) in the multivariate Itô diffusion process as follows.

Definition 2.1. We define the multivariate overnight GARCH-Itô (MOGI) model. In the proposed model, the log price $\mathbf{X}(t)$ and its instantaneous volatility process Σ_t satisfy

$$d\mathbf{X}(t) = \boldsymbol{\mu}dt + \boldsymbol{\sigma}_t^\top d\mathbf{B}_t, \\ \Sigma_t = \begin{cases} \Sigma_{[t]} + \left(\frac{t-[t]}{\tau}\right)^2 \gamma_H (\boldsymbol{\omega}_{H1} + \Sigma_{[t]}) \gamma_H^\top - \frac{t-[t]}{\tau} (\boldsymbol{\omega}_{H2} + \Sigma_{[t]}) \\ + \tau^{-1} \beta_H \int_{[t]}^t \Sigma_s ds \beta_H^\top + \tau^{-2} ([t] + \tau - t) \boldsymbol{\nu} \mathbf{Z}_t \mathbf{Z}_t^\top \boldsymbol{\nu}^\top, & \text{if } t \in ([t], \tau + [t]), \\ \Sigma_{\tau+[t]} + \left(\frac{t-[t]-\tau}{1-\tau}\right)^2 \gamma_L (\boldsymbol{\omega}_{L1} + \Sigma_{\tau+[t]}) \gamma_L^\top \\ - \frac{t-[t]-\tau}{1-\tau} (\boldsymbol{\omega}_{L2} + \Sigma_{\tau+[t]}) + (1-\tau)^{-1} \beta_L \mathbf{r}_t \mathbf{r}_t^\top \beta_L^\top, & \text{if } t \in [\tau + [t], [t] + 1), \end{cases} \quad (2.1)$$

where $[t]$ denotes the integer part of t except that $[t] = t - 1$ when t is an integer, τ is the length of the market open-to-close period, $\mathbf{Z}_t = \int_{[t]}^t d\tilde{\mathbf{B}}_s$, $\mathbf{r}_t = (r_{i,t})_{i=1,\dots,p} = \int_{[t]+\tau}^t \boldsymbol{\sigma}_s^\top d\mathbf{B}_s$, $\tilde{\mathbf{B}}_t$ is a p -dimensional standard Brownian motion with $d\tilde{\mathbf{B}}_t d\mathbf{B}_t = \boldsymbol{\rho} dt$ a.s., $\boldsymbol{\omega}_{H1}$, $\boldsymbol{\omega}_{H2}$, $\boldsymbol{\omega}_{L1}$, and $\boldsymbol{\omega}_{L2}$ are a positive definite p -by- p matrix, and $\boldsymbol{\nu}$, β_H , β_L , γ_H and γ_L are p -by- p symmetric matrices.

The MOGI model has a continuous instantaneous volatility process concerning time t , and it obeys the standard BEKK (1,1) model structure with both the open-to-close integrated volatility matrix and the close-to-open squared log returns as innovations. For example, for $n \in \mathbb{N}$, the instantaneous volatility at the market opening is as follows:

$$\Sigma_n = \boldsymbol{\omega}_L + \gamma_L \boldsymbol{\omega}_H \gamma_L^\top + \gamma_L \gamma_H \Sigma_{n-1} \gamma_H^\top \gamma_L^\top + \tau^{-1} \gamma_L \beta_H \int_{n-1}^{\tau+n-1} \Sigma_t dt \beta_H^\top \gamma_L^\top \\ + (1-\tau)^{-1} \beta_L \mathbf{r}_n \mathbf{r}_n^\top \beta_L^\top,$$

where $\boldsymbol{\omega}_H = \gamma_H \boldsymbol{\omega}_{H1} \gamma_H^\top - \boldsymbol{\omega}_{H2}$, $\boldsymbol{\omega}_L = \gamma_L \boldsymbol{\omega}_{L1} \gamma_L^\top - \boldsymbol{\omega}_{L2}$, and, at the market closing, is as follows:

$$\Sigma_{\tau+n} = \boldsymbol{\omega}_H + \gamma_H \boldsymbol{\omega}_L \gamma_H^\top + \gamma_H \gamma_L \Sigma_{\tau+n-1} \gamma_L^\top \gamma_H^\top + \tau^{-1} \beta_H \int_n^{\tau+n} \Sigma_t dt \beta_H^\top \\ + (1-\tau)^{-1} \gamma_H \beta_L \mathbf{r}_n \mathbf{r}_n^\top \beta_L^\top \gamma_H^\top.$$

Moreover, the instantaneous volatility process can reflect the intraday U-shape trading pat-

tern (Admati and Pfleiderer, 1988; Andersen et al., 1997, 2019; Hong and Wang, 2000) by employing the quadratic interpolation form.

For statistical inference, we study the integrated volatilities obtained from the MOGI model over consecutive integers, and during market opening and closing periods.

Theorem 2.1. *We have the following integrated volatility structures for the proposed MOGI model.*

(a) *For $\det(\beta_H) \neq 0$ and $\|\beta_H\|_2 < 1$, we have*

$$\int_{n-1}^{\tau+n-1} \text{vec}(\Sigma_t) dt = \tau \mathbf{h}_n^H(\theta) + \mathbf{Q}_n^H \text{ a.s.},$$

$$\mathbf{h}_n^H(\theta) = \text{vec}(\omega_H^g) + \mathbf{R}_H^g \mathbf{h}_{n-1}^H(\theta) + \frac{\mathbf{A}_H^g}{\tau} \int_{n-2}^{\tau+n-2} \text{vec}(\Sigma_t) dt + \frac{\mathbf{B}_H^g}{1-\tau} \text{vec}(\mathbf{r}_{n-1} \mathbf{r}_{n-1}^\top),$$

where $\mathbf{R}_H = \gamma_H \otimes \gamma_H$, $\mathbf{B}_H = \beta_H \otimes \beta_H$, \mathbf{I}_{p^2} is a p^2 -dimensional identity matrix, $e^{\mathbf{B}} = \sum_{k=0}^{\infty} \mathbf{B}^k / k!$, $\mathbf{Q}_{H1} = \mathbf{B}_H^{-1}(e^{\mathbf{B}_H} - \mathbf{I}_{p^2})$, $\mathbf{Q}_{H2} = \mathbf{B}_H^{-2}(e^{\mathbf{B}_H} - \mathbf{I}_{p^2} - \mathbf{B}_H)$, $\mathbf{Q}_{H3} = \mathbf{B}_H^{-3}(e^{\mathbf{B}_H} - \mathbf{I}_{p^2} - \mathbf{B}_H - \mathbf{B}_H^2/2)$, $\mathbf{Q}_H = 2\mathbf{Q}_{H3}\mathbf{R}_H + \mathbf{Q}_{H1} - \mathbf{Q}_{H2}$, $\text{vec}(\omega_H^g) = (\mathbf{I}_{p^2} - \mathbf{Q}_H \mathbf{R}_L \mathbf{R}_H \mathbf{Q}_H^{-1}) \{2\mathbf{Q}_{H3}\mathbf{R}_H \text{vec}(\omega_{H1}) - \mathbf{Q}_{H2} \text{vec}(\omega_{H2}) + (\mathbf{Q}_{H2} - 2\mathbf{Q}_{H3}) \text{vec}(\nu \nu^\top)\} + \mathbf{Q}_H \text{vec}(\omega_L) + \mathbf{Q}_H \mathbf{R}_L \text{vec}(\omega_H)$, $\mathbf{R}_H^g = \mathbf{Q}_H \mathbf{R}_L \mathbf{R}_H \mathbf{Q}_H^{-1}$, $\mathbf{A}_H^g = \mathbf{Q}_H \mathbf{R}_L \mathbf{B}_H$, $\mathbf{B}_H^g = \mathbf{Q}_H \mathbf{B}_L$, $A_{k,ij} = \int_{n-1}^{\tau+n-1} \frac{(\tau+n-1-t)^{k+2}}{(k+2) \times k!} Z_{i,t} dZ_{j,t}$, and

$$\mathbf{Q}_n^H = \frac{\nu \otimes \nu}{\tau^2} \sum_{k=0}^{\infty} \tau^{-k} \mathbf{B}_H^k \text{vec} \left((A_{k,ij} + A_{k,ji})_{i,j=1,\dots,p} \right)$$

is a martingale difference.

(b) *For $\det(\beta_L) \neq 0$ and $\|\beta_L\|_2 < 1$, we have*

$$\int_{\tau+n-1}^n \text{vec}(\Sigma_t) dt = (1-\tau) \mathbf{h}_n^L(\theta) + \mathbf{Q}_n^L \text{ a.s.},$$

$$\mathbf{h}_n^L(\theta) = \text{vec}(\omega_L^g) + \mathbf{R}_L^g \mathbf{h}_{n-1}^L(\theta) + \frac{\mathbf{A}_L^g}{\tau} \int_{n-1}^{\tau+n-1} \text{vec}(\Sigma_t) dt + \frac{\mathbf{B}_L^g}{1-\tau} \text{vec}(\mathbf{r}_{n-1} \mathbf{r}_{n-1}^\top),$$

where $\mathbf{R}_L = \gamma_L \otimes \gamma_L$, $\mathbf{B}_L = \beta_L \otimes \beta_L$, $\mathbf{Q}_{L1} = \mathbf{B}_L^{-1}(e^{\mathbf{B}_L} - \mathbf{I}_{p^2})$, $\mathbf{Q}_{L2} = \mathbf{B}_L^{-2}(e^{\mathbf{B}_L} - \mathbf{I}_{p^2} - \mathbf{B}_L)$, $\mathbf{Q}_{L3} = \mathbf{B}_L^{-3}(e^{\mathbf{B}_L} - \mathbf{I}_{p^2} - \mathbf{B}_L - \mathbf{B}_L^2/2)$, $\mathbf{Q}_L = 2\mathbf{Q}_{L3}\mathbf{R}_L + \mathbf{Q}_{L1} - \mathbf{Q}_{L2}$, $\text{vec}(\omega_L^g) = (\mathbf{I}_{p^2} - \mathbf{Q}_L \mathbf{R}_H \mathbf{R}_L \mathbf{Q}_L^{-1}) \{2\mathbf{Q}_{L3}\mathbf{R}_L \text{vec}(\omega_{L1}) - \mathbf{Q}_{L2} \text{vec}(\omega_{L2})\} + \mathbf{Q}_L \text{vec}(\omega_H) + \mathbf{Q}_L \mathbf{R}_H \text{vec}(\omega_L)$,

$$\mathbf{R}_L^g = \boldsymbol{\varrho}_L \mathbf{R}_H \mathbf{R}_L \boldsymbol{\varrho}_L^{-1}, \mathbf{A}_L^g = \boldsymbol{\varrho}_L \mathbf{B}_H, \mathbf{B}_L^g = \boldsymbol{\varrho}_L \mathbf{R}_H \mathbf{B}_L,$$

$$\mathbf{Q}_n = \sum_{k=1}^{\infty} \left(\frac{\mathbf{B}_L}{1-\tau} \right)^k \text{vec} \left(\left(\int_{\tau+n-1}^n \frac{(n-t)^k}{k!} r_{i,t} dr_{j,t} + \int_{\tau+n-1}^n \frac{(n-t)^k}{k!} r_{j,t} dr_{i,t} \right)_{i,j=1,\dots,p} \right)$$

is a martingale difference.

(c) For $\det(\boldsymbol{\beta}_H) \neq 0$, $\det(\boldsymbol{\beta}_L) \neq 0$, $\|\boldsymbol{\beta}_H\|_2 < 1$, and $\|\boldsymbol{\beta}_L\|_2 < 1$, we have

$$\int_{n-1}^n \text{vec}(\boldsymbol{\Sigma}_t) dt = \mathbf{h}_n(\boldsymbol{\theta}) + \mathbf{Q}_n \text{ a.s.},$$

$$\mathbf{h}_n(\boldsymbol{\theta}) = \text{vec}(\boldsymbol{\omega}^g) + \mathbf{R}^g \mathbf{h}_{n-1}(\boldsymbol{\theta}) + \frac{\mathbf{A}^g}{\tau} \int_{n-2}^{\tau+n-2} \text{vec}(\boldsymbol{\Sigma}_t) dt + \frac{\mathbf{B}^g}{1-\tau} \text{vec}(\mathbf{r}_{n-1} \mathbf{r}_{n-1}^\top),$$

$$\text{where } \mathbf{Q}_n = ((1-\tau)\tau^{-1} \boldsymbol{\varrho}_L \mathbf{B}_H + \mathbf{I}_{p^2}) \mathbf{Q}_n^H + \mathbf{Q}_n^L, \boldsymbol{\varrho} = \tau \boldsymbol{\varrho}_H + (1-\tau)(\boldsymbol{\varrho}_L \mathbf{R}_H + \boldsymbol{\varrho}_L \mathbf{B}_H \boldsymbol{\varrho}_H),$$

$$\text{vec}(\boldsymbol{\omega}^g) = (\mathbf{I}_{p^2} - \boldsymbol{\varrho} \mathbf{R}_L \mathbf{R}_H \boldsymbol{\varrho}^{-1}) [\{(1-\tau) \boldsymbol{\varrho}_L \mathbf{B}_H + \tau \mathbf{I}_{p^2}\} \{2 \boldsymbol{\varrho}_{H3} \mathbf{R}_H \text{vec}(\boldsymbol{\omega}_{H1}) - \boldsymbol{\varrho}_{H2} \text{vec}(\boldsymbol{\omega}_{H2}) +$$

$$(\boldsymbol{\varrho}_{H2} - 2 \boldsymbol{\varrho}_{H3}) \text{vec}(\boldsymbol{\nu} \boldsymbol{\nu}^\top)\} + (1-\tau) \{2 \boldsymbol{\varrho}_{L3} \mathbf{R}_L \text{vec}(\boldsymbol{\omega}_{L1}) - \boldsymbol{\varrho}_{L2} \text{vec}(\boldsymbol{\omega}_{L2})\} + (1-\tau) \boldsymbol{\varrho}_L \text{vec}(\boldsymbol{\omega}_H)] +$$

$$\boldsymbol{\varrho} \text{vec}(\boldsymbol{\omega}_L) + \boldsymbol{\varrho} \mathbf{R}_L \text{vec}(\boldsymbol{\omega}_H), \mathbf{R}^g = \boldsymbol{\varrho} \mathbf{R}_L \mathbf{R}_H \boldsymbol{\varrho}^{-1}, \mathbf{A}^g = \boldsymbol{\varrho} \mathbf{R}_L \mathbf{B}_H, \mathbf{B}^g = \boldsymbol{\varrho} \mathbf{B}_L.$$

Theorem 2.1 (c) shows that the daily integrated volatility can be decomposed into $\mathbf{h}_n(\boldsymbol{\theta})$ and \mathbf{Q}_n , where $\mathbf{h}_n(\boldsymbol{\theta})$ is adapted to the filtration, $\mathcal{F}_{n-1} = \sigma(\mathbf{X}(t), t \leq n-1)$, and \mathbf{Q}_n is the martingale difference. Note that the conditional daily integrated volatility is in the famous VEC-GARCH(1,1) structure (Bollerslev et al., 1988) with the open-to-close integrated volatility and the close-to-open squared log return as innovations. In Section 3, we propose a parameter estimation procedure based on the inherent iterative structure in the integrated volatilities described in Theorem 2.1. However, since we cannot observe the random fluctuation term \mathbf{Z}_t and instantaneous volatility process, the interceptor parameters $\boldsymbol{\omega}_{H1}$, $\boldsymbol{\omega}_{H2}$, $\boldsymbol{\omega}_{L1}$, $\boldsymbol{\omega}_{L2}$, and $\boldsymbol{\nu}$ are hard to be estimated directly. Thus, we develop a parameter estimation procedure for $\boldsymbol{\omega}_H^g$, $\boldsymbol{\omega}_L^g$, $\boldsymbol{\gamma}_H$, $\boldsymbol{\gamma}_L$, $\boldsymbol{\beta}_H$, and $\boldsymbol{\beta}_L$ instead. Moreover, to estimate the interceptor $\boldsymbol{\omega}^g$ for the whole-day dynamics, we use the following expression:

$$\text{vec}(\boldsymbol{\omega}^g) = (\mathbf{I}_{p^2} - \mathbf{R}^g) \left[\{(1-\tau) \mathbf{A}_L^g + \tau \mathbf{I}_{p^2}\} (\mathbf{I}_{p^2} - \mathbf{R}_H^g)^{-1} \text{vec}(\boldsymbol{\omega}_H^g) \right. \\ \left. + (1-\tau) (\mathbf{I}_{p^2} - \mathbf{R}_L^g)^{-1} \text{vec}(\boldsymbol{\omega}_L^g) \right].$$

If instantaneous volatility estimators are available, then we are able to estimate the intercept parameters ω_{H1} , ω_{H2} , ω_{L1} , ω_{L2} . However, this is not the focus of the paper, so we leave it for future study.

3 Parameter estimation procedure

In this section, we present an estimation procedure for the model parameters and establish its asymptotic theorems.

3.1 A model set-up

We assume that the true log price process follows the MOGI model in Definition 2.1. Due to the imperfections of the trading mechanisms, high-frequency data are contaminated by market microstructure noises so that the observed stock prices are in a noisy version of the true stock prices (Aït-Sahalia and Yu, 2009). In contrast, for low-frequency data, the effect of the microstructure noises is negligible, thus, we assume that the true log prices $\mathbf{X}(t)$ and $\mathbf{X}(t + \tau)$, $t = 0, \dots, n$, at the market opening and closing times are observed. In light of this, we assume that the high-frequency intraday observations $\mathbf{X}(t_{k,\ell})$, $\ell = 1, \dots, m - 1$, where $k - 1 = t_{k,0} < \dots < t_{k,m} = k - 1 + \tau$, are masked by the microstructure noises as follows:

$$Y_i(t_{k,\ell}) = X_i(t_{k,\ell}) + \epsilon_i(t_{k,\ell}), \quad i = 1, \dots, p, k = 1, \dots, n, \ell = 1, \dots, m - 1, \quad (3.1)$$

where the microstructure noises ϵ_i 's are independent random variables with mean zero and variance η_{ii} . The noises are also independent of the price and volatility processes. For simplicity, we assume that the data are synchronized and the observed time points $t_{k,\ell}$'s are equally spaced, that is, $t_{k,\ell} - t_{k,\ell-1} = m^{-1}$ for $k = 1, \dots, n$ and $\ell = 1, \dots, m$.

Remark 3.1. In practice, for the multivariate stock price process, high-frequency data are not synchronized, while observed time points are not equally spaced. This is the so-called non-synchronization problem and has been well studied in the finance literature. Data synchronization schemes include the refresh time (Barndorff-Nielsen et al., 2011), the pre-

vious tick time (Wang and Zou, 2010; Zhang, 2011), and the generalized sampling time (Aït-Sahalia et al., 2010). Under some mild conditions, these schemes provide the tools for solving the non-synchronization problem and to further obtain estimators for the daily integrated volatility given high-frequency data (Aït-Sahalia et al., 2010; Barndorff-Nielsen et al., 2011; Bibinger et al., 2014; Christensen et al., 2010; Wang and Zou, 2010; Zhang, 2011). To highlight the modeling of the parametric volatility process, we make the simple assumption that the high-frequency observations are equally spaced and synchronized.

Given high-frequency data from the market open-to-close period, we can estimate the integrated volatility $\int_{n-1}^{\tau+n-1} \text{vec}(\Sigma_t) dt$ with the realized volatility matrix estimators, such as the multi-scale realized volatility matrix (MSRVM) (Zhang, 2011), the pre-averaging realized volatility matrix (PRVM) (Christensen et al., 2010), and the kernel realized volatility matrix (KRVM) (Barndorff-Nielsen et al., 2011). See also Aït-Sahalia et al. (2010); Barndorff-Nielsen et al. (2008); Bibinger et al. (2014); Fan and Wang (2007); Fan and Kim (2018); Jacod et al. (2009); Kim et al. (2018); Xiu (2010); Zhang (2006); Wang and Zou (2010) for related research works. These non-parametric realized volatility matrix estimators can estimate historical volatility well. Moreover, as the number of high-frequency observations m goes to infinity, the majority of these non-parametric estimators can achieve the optimal convergence rate of $m^{-1/4}$ for estimating the open-to-close integrated volatility matrix in the presence of market microstructure noises. In this paper, we denote such estimators by RV_k , $k = 1, \dots, n$, while in the numerical study, we use the PRVM estimator with weight function $\max(x, 1 - x)$.

3.2 Weighted least squares estimation

In this section, we propose a quasi-maximum likelihood estimation procedure to estimate the true parameter $\theta_0 = (\text{vech}(\omega_{H0}^g), \text{vech}(\omega_{L0}^g), \text{vech}(\gamma_{H0}), \text{vech}(\gamma_{L0}), \text{vech}(\beta_{H0}), \text{vech}(\beta_{L0}), \mu_0)$ of the MOGI model and establish its asymptotic behavior. Let d be the cardinality of θ , that is, $d = |\theta|$. We note that ρ does not have a role to define the conditional expected volatility matrix; thus, we do not include ρ in the parameter of interest.

To estimate the model parameters, we examine the volatility dynamics during the open-

to-close and close-to-open periods separately and, then, draw combined inferences. Specifically, the integrated volatilities hold the following relationships (see Theorem 2.1):

$$\begin{aligned} \int_{n-1}^{\tau+n-1} \text{vec}(\boldsymbol{\Sigma}_t) dt &= \tau \mathbf{h}_n^H(\boldsymbol{\theta}_0) + \mathbf{Q}_n^H, \\ \int_{\tau+n-1}^n \text{vec}(\boldsymbol{\Sigma}_t) dt &= (1 - \tau) \mathbf{h}_n^L(\boldsymbol{\theta}_0) + \mathbf{Q}_n^L \text{ a.s.} \end{aligned}$$

For the open-to-close period, we can estimate the integrated volatility well with the MSRV, the PRVM, or the KRVM. For the close-to-open period, high-frequency data are not available so that we approximate the integrated volatility with the close-to-open squared log return. Specifically, Itô's lemma provides

$$\text{vec}(\mathbf{r}_n(\boldsymbol{\mu})\mathbf{r}_n(\boldsymbol{\mu})^\top) = (1 - \tau) \mathbf{h}_n^L(\boldsymbol{\theta}_0) + \mathbf{Q}_n^{LL} \text{ a.s.},$$

where $\mathbf{Q}_n^{LL} = \mathbf{Q}_n^L + \left(\int_{\tau+n-1}^n r_{i,t} dr_{j,t} + \int_{\tau+n-1}^n r_{j,t} dr_{i,t} \right)_{i,j=1,\dots,p}$ and $\mathbf{r}_n(\boldsymbol{\mu}) = \mathbf{X}(n) - \mathbf{X}(\tau + n - 1) - (1 - \tau)\boldsymbol{\mu}$. Thus, we can use the realized volatility estimators RV_n and the close-to-open squared log returns $\mathbf{r}_n(\boldsymbol{\mu})\mathbf{r}_n(\boldsymbol{\mu})^\top$ as proxies for the open-to-close and close-to-open conditional volatilities, respectively. The accuracy of the proxies can be measured by the variance of the martingale differences \mathbf{Q}_n^H and \mathbf{Q}_n^{LL} . To reflect the variance information on the estimation procedure, we adopt the famous weighted square loss function as follows:

$$\begin{aligned} L_n(\boldsymbol{\theta}) &= \frac{1}{2n} \sum_{k=1}^n \left[\left\{ \text{vech}(IV_k) - \tau \mathbf{h}_{h,k}^H(\boldsymbol{\theta}) \right\}^\top \mathbf{V}_H^{-1} \left\{ \text{vech}(IV_k) - \tau \mathbf{h}_{h,k}^H(\boldsymbol{\theta}) \right\} \right. \\ &\quad \left. + \left\{ \mathbf{r}_{h,k}^2(\boldsymbol{\mu}) - (1 - \tau) \mathbf{h}_{h,k}^L(\boldsymbol{\theta}) \right\}^\top \mathbf{V}_L^{-1} \left\{ \mathbf{r}_{h,k}^2(\boldsymbol{\mu}) - (1 - \tau) \mathbf{h}_{h,k}^L(\boldsymbol{\theta}) \right\} \right], \end{aligned}$$

where \mathbf{V}_H and \mathbf{V}_L are covariance matrices for the \mathbf{Q}_n^H and \mathbf{Q}_n^{LL} terms, respectively. Moreover, $IV_k = \int_{k-1}^{\tau+k-1} \boldsymbol{\Sigma}_t dt$, $\mathbf{h}_{h,n}^H(\boldsymbol{\theta}) = \text{vech}(\text{vec}^{-1}(\mathbf{h}_n^H(\boldsymbol{\theta})))$, $\mathbf{h}_{h,n}^L(\boldsymbol{\theta}) = \text{vech}(\text{vec}^{-1}(\mathbf{h}_n^L(\boldsymbol{\theta})))$, and $\mathbf{r}_{h,k}^2(\boldsymbol{\mu}) = \text{vech}(\mathbf{r}_k(\boldsymbol{\mu})\mathbf{r}_k(\boldsymbol{\mu})^\top)$. Since the integrated volatilities IV_k 's during the open-to-close period are not observable, we harness its well-performing realized volatility matrix

estimators RV_k 's to obtain the conditional volatilities in the following:

$$\begin{aligned}\widehat{\mathbf{h}}_n^H(\boldsymbol{\theta}) &= \text{vec}(\boldsymbol{\omega}_H^g) + \mathbf{R}_H^g \widehat{\mathbf{h}}_{n-1}^H(\boldsymbol{\theta}) + \frac{\mathbf{A}_H^g}{\tau} \text{vec}(RV_{n-1}) + \frac{\mathbf{B}_H^g}{1-\tau} \text{vec}(\mathbf{r}_{n-1}(\boldsymbol{\mu}) \mathbf{r}_{n-1}^\top(\boldsymbol{\mu})), \\ \widehat{\mathbf{h}}_n^L(\boldsymbol{\theta}) &= \text{vec}(\boldsymbol{\omega}_L^g) + \mathbf{R}_L^g \widehat{\mathbf{h}}_{n-1}^L(\boldsymbol{\theta}) + \frac{\mathbf{A}_L^g}{\tau} \text{vec}(RV_n) + \frac{\mathbf{B}_L^g}{1-\tau} \text{vec}(\mathbf{r}_{n-1}(\boldsymbol{\mu}) \mathbf{r}_{n-1}^\top(\boldsymbol{\mu})).\end{aligned}$$

The weighted square loss function is estimated by

$$\begin{aligned}\widehat{L}_{n,m}(\boldsymbol{\theta}) &= \frac{1}{2n} \sum_{k=1}^n \left[\left\{ \text{vech}(RV_k) - \tau \widehat{\mathbf{h}}_{h,k}^H(\boldsymbol{\theta}) \right\}^\top \widehat{\mathbf{V}}_H^{-1} \left\{ \text{vech}(RV_k) - \tau \widehat{\mathbf{h}}_{h,k}^H(\boldsymbol{\theta}) \right\} \right. \\ &\quad \left. + \left\{ \mathbf{r}_{h,k}^2(\boldsymbol{\mu}) - (1-\tau) \widehat{\mathbf{h}}_{h,k}^L(\boldsymbol{\theta}) \right\}^\top \widehat{\mathbf{V}}_L^{-1} \left\{ \mathbf{r}_{h,k}^2(\boldsymbol{\mu}) - (1-\tau) \widehat{\mathbf{h}}_{h,k}^L(\boldsymbol{\theta}) \right\} \right],\end{aligned}\tag{3.2}$$

where $\widehat{\mathbf{h}}_{h,n}^H(\boldsymbol{\theta}) = \text{vech}\left(\text{vec}^{-1}\left(\widehat{\mathbf{h}}_n^H(\boldsymbol{\theta})\right)\right)$, $\widehat{\mathbf{h}}_{h,n}^L(\boldsymbol{\theta}) = \text{vech}\left(\text{vec}^{-1}\left(\widehat{\mathbf{h}}_n^L(\boldsymbol{\theta})\right)\right)$, and $\widehat{\mathbf{V}}_H$ and $\widehat{\mathbf{V}}_L$ are some consistent estimators for \mathbf{V}_H and \mathbf{V}_L , which are proposed in Section 3.3. The true parameter $\boldsymbol{\theta}$ is estimated by minimizing $\widehat{L}_{n,m}(\boldsymbol{\theta})$, that is,

$$\widehat{\boldsymbol{\theta}} = \arg \min_{\boldsymbol{\theta} \in \boldsymbol{\Theta}} \widehat{L}_{n,m}(\boldsymbol{\theta}),$$

where $\boldsymbol{\Theta}$ is the parameter space of $\boldsymbol{\theta}$. We call it the weighted least square estimator (WLSE).

To establish the asymptotic theorems for the proposed WLSE $\widehat{\boldsymbol{\theta}}$, we require the following conditions.

Assumption 3.1.

- (a) $\boldsymbol{\Theta}$ is compact; $\boldsymbol{\omega}_H^g$ and $\boldsymbol{\omega}_L^g$ are positive definite; $\boldsymbol{\beta}_H$, $\boldsymbol{\beta}_L$, $\boldsymbol{\gamma}_H$ and $\boldsymbol{\gamma}_L$ are lower triangle matrices; their (1,1)th elements are restricted to be positive; $\|\boldsymbol{\beta}_H\|_2$, $\|\boldsymbol{\beta}_L\|_2$, $\|\boldsymbol{\gamma}_H\|_2$ and $\|\boldsymbol{\gamma}_L\|_2$ are less than 1; $\boldsymbol{\theta}_0$ is an interior point of $\boldsymbol{\Theta}$;
- (b) The spot volatility process has the finite 8th moment;
- (c) $\max_k E[\|RV_k - IV_k\|_F^4] = O(p^4 m^{-1})$;
- (d) $\widehat{\mathbf{V}}_H$ and $\widehat{\mathbf{V}}_L$ are strictly positive definite and consistent estimators for \mathbf{V}_H and \mathbf{V}_L ;
- (e) $(IV_k, \mathbf{r}_k, \mathbf{Q}_k^H, \mathbf{Q}_k^{LL})$ is a stationary ergodic process, and $nm^{-1/2} \rightarrow 0$;

Remark 3.2. Under the finite fourth moment condition, Kim et al. (2016) showed that the realized volatility estimators satisfy Assumption 3.1(c). When we use the eigenvectors of the volatility matrix estimators as $\widehat{\mathbf{V}}_H$ and $\widehat{\mathbf{V}}_L$, Assumption 3.1(d) is satisfied. The condition in Assumption 3.1(e) is required to study the asymptotic distribution of the proposed WLSE $\widehat{\boldsymbol{\theta}}$. For example, the stationary condition is required to derive the asymptotic normality (see Theorem 3.2). Furthermore, the condition $nm^{-1/2} \rightarrow 0$ is imposed so that the high-frequency estimation errors of order $m^{-1/4}$ are negligible in comparison with the low-frequency estimation errors of order $n^{-1/2}$.

The following theorems present the asymptotic results for the proposed WLSE $\widehat{\boldsymbol{\theta}}$.

Theorem 3.1. *Under Assumption 3.1(a)–(d) and for $n \geq d$, we have*

$$\left\| \widehat{\boldsymbol{\theta}} - \boldsymbol{\theta}_0 \right\|_{\max} = O_p(m^{-1/4} + n^{-1/2}).$$

Theorem 3.2. *Under Assumption 3.1, we have as $n, m \rightarrow \infty$,*

$$n^{1/2} \left(\widehat{\boldsymbol{\theta}} - \boldsymbol{\theta}_0 \right) \xrightarrow{d} \mathcal{MN} \left(0, \mathbf{B}^{-1} \mathbf{A} \mathbf{B}^{-1} \right),$$

where $\mathbf{A} = \mathbf{A}_H + \mathbf{A}_L$, $\mathbf{B} = \mathbf{B}_H + \mathbf{B}_L$,

$$\begin{aligned} \mathbf{A}_H &= E \left[\frac{\partial \tau \mathbf{h}_{h,1}^H(\boldsymbol{\theta})}{\partial \boldsymbol{\theta}} \mathbf{V}_H^{-1} \mathbf{Q}_{h,1}^H \mathbf{Q}_{h,1}^{H\top} \mathbf{V}_H^{-1} \frac{\partial \tau \mathbf{h}_{h,1}^H(\boldsymbol{\theta})}{\partial \boldsymbol{\theta}^\top} \Big|_{\boldsymbol{\theta}=\boldsymbol{\theta}_0} \right], \\ \mathbf{A}_L &= E \left[\frac{\partial \mathbf{r}_{h,1}^2(\boldsymbol{\mu}) - (1 - \tau) \mathbf{h}_{h,1}^L(\boldsymbol{\theta})}{\partial \boldsymbol{\theta}} \mathbf{V}_L^{-1} \mathbf{Q}_{h,1}^{LL} \mathbf{Q}_{h,1}^{LL\top} \mathbf{V}_L^{-1} \frac{\partial \mathbf{r}_{h,1}^2(\boldsymbol{\mu}) - (1 - \tau) \mathbf{h}_{h,1}^L(\boldsymbol{\theta})}{\partial \boldsymbol{\theta}^\top} \Big|_{\boldsymbol{\theta}=\boldsymbol{\theta}_0} \right], \\ \mathbf{B}_H &= 2E \left[\frac{\partial \tau \mathbf{h}_{h,1}^H(\boldsymbol{\theta})}{\partial \boldsymbol{\theta}} \mathbf{V}_H^{-1} \frac{\partial \tau \mathbf{h}_{h,1}^H(\boldsymbol{\theta})}{\partial \boldsymbol{\theta}^\top} \Big|_{\boldsymbol{\theta}=\boldsymbol{\theta}_0} \right], \\ \mathbf{B}_L &= 2E \left[\frac{\partial \mathbf{r}_{h,1}^2(\boldsymbol{\mu}) - (1 - \tau) \mathbf{h}_{h,1}^L(\boldsymbol{\theta})}{\partial \boldsymbol{\theta}} \mathbf{V}_L^{-1} \frac{\partial \mathbf{r}_{h,1}^2(\boldsymbol{\mu}) - (1 - \tau) \mathbf{h}_{h,1}^L(\boldsymbol{\theta})}{\partial \boldsymbol{\theta}^\top} \Big|_{\boldsymbol{\theta}=\boldsymbol{\theta}_0} \right], \\ \mathbf{Q}_{h,1}^H &= \text{vech}(IV_1) - \tau \mathbf{h}_{h,1}^H(\boldsymbol{\theta}_0), \quad \text{and} \quad \mathbf{Q}_{h,1}^{LL} = \mathbf{r}_{h,1}^2(\boldsymbol{\mu}_0) - (1 - \tau) \mathbf{h}_{h,1}^L(\boldsymbol{\theta}_0). \end{aligned}$$

Remark 3.3. Theorem 3.1 shows that the convergence rate of the WLSE $\widehat{\boldsymbol{\theta}}$ is $m^{-1/4} + n^{-1/2}$. The first term $m^{-1/4}$ is the cost to estimate open-to-close integrated volatilities, which is

known as the optimal convergence rate in the presence of market microstructure noises. The second term $n^{-1/2}$ is the usual parametric convergence rate based on the low-frequency structure. Theorem 3.2 shows the asymptotic normality of the WLSE $\widehat{\boldsymbol{\theta}}$.

3.3 Choice of weight matrices for the WLSE

The performance of the proposed WLSE procedure depends on the choice of the weight matrices \mathbf{V}_H and \mathbf{V}_L . The optimal choice of the weight matrices \mathbf{V}_H and \mathbf{V}_L minimizes the asymptotic variance $\mathbf{B}^{-1}\mathbf{A}\mathbf{B}^{-1}$ in Theorem 3.2, which is a function of the variances of the martingale difference terms. Thus, the weight matrices \mathbf{V}_H and \mathbf{V}_L can be determined by the variances of the martingale difference terms. For example, for the open-to-close period, the difference between the GARCH volatility $\tau \mathbf{h}_{h,k}^H(\boldsymbol{\theta}_0)$ and the proxy $\text{vech}(IV_k)$ is $\mathbf{Q}_{h,k}^H$, while, for the close-to-open period, the difference between the GARCH volatility $(1 - \tau) \mathbf{h}_{h,k}^L(\boldsymbol{\theta}_0)$ and the proxy $\text{vech}(\mathbf{r}_{k-1} \mathbf{r}_{k-1}^\top)$ is $\mathbf{Q}_{h,k}^L$. Then \mathbf{V}_H and \mathbf{V}_L are the covariance matrices of the martingale differences $\mathbf{Q}_{h,k}^H$ and $\mathbf{Q}_{h,k}^L$, respectively. To estimate the variance of the martingale difference terms, we first estimate the GARCH volatilities for the open-to-close and close-to-open periods separately. Specifically, we estimate the GARCH parameters $\boldsymbol{\theta}_{H,0}^g = (\text{vech}(\boldsymbol{\omega}_{H0}^g), \text{vec}(\mathbf{R}_{H0}^g), \text{vec}(\mathbf{A}_{H0}^g), \text{vec}(\mathbf{B}_{H0}^g), \boldsymbol{\mu}_0)$ and $\boldsymbol{\theta}_{L,0}^g = (\text{vech}(\boldsymbol{\omega}_{L0}^g), \text{vec}(\mathbf{R}_{L0}^g), \text{vec}(\mathbf{A}_{L0}^g), \text{vec}(\mathbf{B}_{L0}^g), \boldsymbol{\mu}_0)$ by

$$\widehat{\boldsymbol{\theta}}_H^g = \arg \min_{\boldsymbol{\theta}_H^g} \frac{1}{2n} \sum_{k=1}^n \left\{ \text{vech}(RV_k) - \tau \widehat{\mathbf{h}}_{h,k}^H(\boldsymbol{\theta}) \right\}^\top \left\{ \text{vech}(RV_k) - \tau \widehat{\mathbf{h}}_{h,k}^H(\boldsymbol{\theta}) \right\}$$

and

$$\widehat{\boldsymbol{\theta}}_L^g = \arg \min_{\boldsymbol{\theta}_L^g} \frac{1}{2n} \sum_{k=1}^n \left\{ \mathbf{r}_{h,k}^2(\boldsymbol{\mu}) - (1 - \tau) \widehat{\mathbf{h}}_{h,k}^L(\boldsymbol{\theta}) \right\}^\top \left\{ \mathbf{r}_{h,k}^2(\boldsymbol{\mu}) - (1 - \tau) \widehat{\mathbf{h}}_{h,k}^L(\boldsymbol{\theta}) \right\}.$$

Similar to Theorem 3.1, we can show that the least squares estimators (LSE) $\widehat{\boldsymbol{\theta}}_H^g$ and $\widehat{\boldsymbol{\theta}}_L^g$ are consistent with the convergence rate $n^{-1/2} + m^{-1/4}$ under Assumption 3.1. Then, with these

consistent estimators, we calculate their sample covariances as follows:

$$\begin{aligned}\tilde{\mathbf{V}}_H &= \frac{1}{n} \sum_{k=1}^n \left\{ \text{vech}(RV_k) - \tau \hat{\mathbf{h}}_{h,k}^H(\hat{\boldsymbol{\theta}}_H^g) \right\} \left\{ \text{vech}(RV_k) - \tau \hat{\mathbf{h}}_{h,k}^H(\hat{\boldsymbol{\theta}}_H^g) \right\}^\top, \\ \tilde{\mathbf{V}}_L &= \frac{1}{n} \sum_{k=1}^n \left\{ \mathbf{r}_{h,k}^2(\hat{\boldsymbol{\mu}}_L) - (1 - \tau) \hat{\mathbf{h}}_{h,k}^L(\hat{\boldsymbol{\theta}}_L^g) \right\} \left\{ \mathbf{r}_{h,k}^2(\hat{\boldsymbol{\mu}}_L) - (1 - \tau) \hat{\mathbf{h}}_{h,k}^L(\hat{\boldsymbol{\theta}}_L^g) \right\}^\top. \quad (3.3)\end{aligned}$$

Under the stationary condition, we can show that $\tilde{\mathbf{V}}_H$ and $\tilde{\mathbf{V}}_L$ converge to their corresponding covariance matrices using the martingale convergence theorem. Due to the estimation errors from the finite sample estimation, some eigenvalues of the estimated weight matrices can be too small, which makes the estimators of the inverse weight matrices unstable. We therefore added a small positive value to the eigenvalues of the weight matrices. Specifically, we employed consistent estimators of \mathbf{V}_H and \mathbf{V}_L as follows:

$$\hat{\mathbf{V}}_H = \tilde{\mathbf{V}}_H + v_n^H \mathbf{I}_{p(p-1)/2} \quad \text{and} \quad \hat{\mathbf{V}}_L = \tilde{\mathbf{V}}_L + v_n^L \mathbf{I}_{p(p-1)/2},$$

where $\tilde{\mathbf{V}}_H$ and $\tilde{\mathbf{V}}_L$ are defined in (3.3), and v_n^H and v_n^L are tuning parameters, converging to zero. In the numerical study, we choose v_n^H and v_n^L as follows:

$$v_n^H = \frac{1}{p(p-1)/2} \sum_{i=1}^{p(p-1)/2} [\tilde{\mathbf{V}}_H]_{ii} n^{-3/5} \quad \text{and} \quad v_n^L = \frac{1}{p(p-1)/2} \sum_{i=1}^{p(p-1)/2} [\tilde{\mathbf{V}}_L]_{ii} n^{-3/5},$$

where $[\mathbf{M}]_{ij}$ denotes the (i, j) th entry of a matrix \mathbf{M} . We note that $\hat{\mathbf{V}}_H$ and $\hat{\mathbf{V}}_L$ are consistent estimators of \mathbf{V}_H and \mathbf{V}_L , which have the same convergence rate as that of $\tilde{\mathbf{V}}_H$ and $\tilde{\mathbf{V}}_L$, respectively, so that all of the asymptotic properties hold with $\hat{\mathbf{V}}_H$ and $\hat{\mathbf{V}}_L$.

We use the estimated weight matrices $\hat{\mathbf{V}}_H$ and $\hat{\mathbf{V}}_L$ to evaluate the weighted square loss function $\hat{L}_{n,m}(\boldsymbol{\theta})$ in (3.2). This procedure helps to assign more weights to the more informative and accurate proxy. Intuitively, the open-to-close period should be more informative given the abundant high-frequency observations, thus, more weight will be assigned to the open-to-close proxy. In the empirical study, $\hat{\mathbf{V}}_H$ is smaller than $\hat{\mathbf{V}}_L$ in terms of eigenvalues. Finally, with the consistent estimators $\hat{\mathbf{V}}_H$ and $\hat{\mathbf{V}}_L$, we can establish the asymptotic results

in Theorems 3.1–3.2.

4 Large volatility matrix inference

4.1 Approximate factor models

In financial applications, we often encounter a large number of assets in asset pricing, portfolio allocation, and risk management problems. Taking the current MOGI model directly to the high-dimensional set-up is not valid, as it results in $O(p^2)$ parameters. Therefore, for a large number of assets, we construct the MOGI model based on the factor Itô diffusion process and assume the model structure described in (2.1) for the instantaneous factor volatility process. Specifically, to account for common market factors in the stock market, we employ the approximate factor models and assume the following factor Itô diffusion process:

$$d\mathbf{X}(t) = \mathbf{U}\boldsymbol{\mu}dt + \mathbf{U}d\mathbf{f}(t) + d\mathbf{u}(t),$$

where $\boldsymbol{\mu} \in \mathbb{R}^r$ is a drift vector, \mathbf{U} is a p -by- r factor loading matrix and r is the total number of market factors that is much smaller than p . Moreover, $\mathbf{f}(t)$ and $\mathbf{u}(t)$ are latent factor and idiosyncratic diffusion processes in the following:

$$d\mathbf{f}(t) = \boldsymbol{\sigma}_t^\top d\mathbf{B}_t \quad \text{and} \quad d\mathbf{u}(t) = \boldsymbol{\vartheta}_t^\top d\mathbf{W}_t,$$

where $\boldsymbol{\sigma}_t$ is an r -by- r matrix, $\boldsymbol{\vartheta}_t$ is a p -by- p matrix, and \mathbf{B}_t and \mathbf{W}_t are independent r -dimensional and p -dimensional Brownian motions, respectively. As a result, the corresponding daily integrated volatility matrix $\boldsymbol{\Gamma}_n$ for the n th day consists of the factor volatility and idiosyncratic volatility matrices

$$\boldsymbol{\Gamma}_n = \boldsymbol{\zeta}_n + \boldsymbol{\Gamma}_n^s,$$

where

$$\boldsymbol{\zeta}_n = \mathbf{U}\boldsymbol{\Psi}_n\mathbf{U}^\top, \quad \boldsymbol{\Psi}_n = \int_{n-1}^n \boldsymbol{\sigma}_t^\top \boldsymbol{\sigma}_t dt \quad \text{and} \quad \boldsymbol{\Gamma}_n^s = \int_{n-1}^n \boldsymbol{\vartheta}_t^\top \boldsymbol{\vartheta}_t dt.$$

The latent factor process $\mathbf{f}(t)$ corresponds to the systematic risk that is known to be undiversifiable, and it is important to model the rich dynamics in the factor volatility Ψ_n process. Thus, we embed the MOGI structure described in (2.1) in the instantaneous factor volatility process to capture the market dynamics. On the other hand, the idiosyncratic process $\mathbf{u}(t)$ corresponds to the firm-specific risk that can be usually mitigated through diversification. Thus, its corresponding volatility matrix Γ_n^s retains a sparse structure and we discuss its estimation in Section 4.3.

In the previous section, for a finite number of assets, we proposed the WLSE for the MOGI model parameters and showed that it has good asymptotic behavior. To ensure the performance of the WLSE for a large number of assets, we need to impose certain structures on the factor loading matrix \mathbf{U} and the factor volatility matrix Ψ_n , as well as on the idiosyncratic volatility matrix Γ_n^s so that they can be estimated consistently. We provide discussions in Sections 4.2 and 4.3.

4.2 Factor loading and volatility matrices

The factor volatility process $\mathbf{f}(t)$ is latent so that we are required to impose certain structures for its identification. Researchers often assume that the factor loading matrix \mathbf{U} is orthogonal while the factor volatility matrix Ψ_k (or $\sigma_t^\top \sigma_t$) is diagonal (Aït-Sahalia and Xiu, 2017; Fan et al., 2013; Kim and Fan, 2019). Under such assumptions, \mathbf{U} and Ψ_k correspond to the eigenmatrix and eigenvalues of the daily integrated volatility matrix Γ_k , respectively. In this case, our proposed MOGI model returns to the factor GARCH-Itô model structure introduced by Kim and Fan (2019), as the factor GARCH-Itô model describes the eigenvalue dynamics of the factor volatility process. Here the diagonal assumption on Ψ_k is rather restrictive in the sense that cross-sectional dynamics cannot be studied. Under such assumptions, the market dynamics only come from each factor marginally, while the correlations among factors are kept stable over time, which makes it difficult to explain the dynamics among factors. On the other hand, Kim et al. (2018) proposed the factor diffusion process to account for the grouping effects. Such grouping effects include sector and industry classifications, in which case one could use the global industry classification standard (GICS)

as the group membership. Specifically, the factor loading matrix $\mathbf{U} = (U_{ij})_{i=1,\dots,p,j=1,\dots,r}$ is the membership matrix, where $U_{i,j}$ is equal to one if the i th asset belongs to the j th factor, and it is equal to zero, otherwise. However, the performance of such models depends on the choice of the group membership. Recently, Kim et al. (2020) suggested that one could estimate the factor loading matrix using the eigenmatrix of the variance from all daily integrated volatility matrices $\mathbf{\Gamma}_k$'s, and this method does not require $\mathbf{\Psi}_k$ to be diagonal. Moreover, the factor loading matrix can be estimated non-parametrically under some stationary conditions, which, however, may be restrictive to model the idiosyncratic volatility matrix. See also Aït-Sahalia and Xiu (2017); Kong (2017, 2018); Kong et al. (2021); Pelger (2019).

As discussed above, each approach has its own advantages and disadvantages, and the factor volatility matrix can be identified as long as the factor loading matrix \mathbf{U} can be well estimated. However, the estimation of \mathbf{U} is not the focus of this paper, and so we depend on existing research in the literature for this part and denote the consistent estimator of \mathbf{U} by $\hat{\mathbf{U}}$.

4.3 Idiosyncratic volatility matrices

The idiosyncratic process $\mathbf{u}(t)$ is related to firm-specific risk so that assets are usually weakly correlated in its corresponding volatility matrix $\mathbf{\Gamma}_k^s$. Therefore, we impose the sparse condition on the idiosyncratic volatility matrix $\mathbf{\Gamma}_k^s = (\Gamma_{k,ij}^s)_{i,j=1,\dots,p}$ as follows:

$$\max_{1 \leq j \leq p} \sum_{i=1}^p |\Gamma_{k,ij}^s|^\delta |\Gamma_{k,ii}^s \Gamma_{k,jj}^s|^{(1-\delta)/2} \leq M\pi(p) \quad \text{a.s.}, \quad (4.1)$$

where $\delta \in [0, 1)$, M is the positive bounded random variable, and the sparsity level $\pi(p)$ diverges very slowly, such as $\log p$ (Aït-Sahalia and Xiu, 2017; Fan and Kim, 2019; Fan et al., 2013, 2016; Kim et al., 2018, 2020; Kong, 2018; Shin et al., 2021). Furthermore, we assume that the idiosyncratic volatility matrix $\mathbf{\Gamma}_k^s$ satisfies

$$\mathbf{\Gamma}_k^s = \mathbf{\Gamma}^s \text{ a.s.} \quad \text{for all } k = 1, \dots, n. \quad (4.2)$$

The constant condition (4.2) is imposed so that the volatility matrices for the open-to-close period can be estimated consistently.

To estimate the sparse idiosyncratic volatility matrix $\mathbf{\Gamma}^s$, we follow the POET procedure introduced by Fan et al. (2013). Specifically, the input integrated volatility matrix estimator is estimated by

$$\widehat{\mathbf{\Gamma}}_n = \frac{1}{n} \sum_{k=1}^n \widehat{\mathbf{\Gamma}}_k^H + \frac{1}{n} \sum_{k=1}^n (\mathbf{X}(k) - \mathbf{X}(\tau + k - 1) - \bar{\mathbf{X}})(\mathbf{X}(k) - \mathbf{X}(\tau + k - 1) - \bar{\mathbf{X}})^\top,$$

where $\widehat{\mathbf{\Gamma}}_k^H$ is the realized volatility matrix estimator, such as the MSRV, the PRV, or the KRV given the k th period open-to-close high-frequency data, and $\bar{\mathbf{X}}$ is the sample mean of all close-to-open log returns. We note that, under some regularity conditions, the input estimator $\widehat{\mathbf{\Gamma}}_n$ converges to $\bar{\mathbf{\Gamma}}_n = \sum_{k=1}^n \mathbf{\Gamma}_k/n$. Then, $\widehat{\mathbf{\Gamma}}_n$ admits

$$\widehat{\mathbf{\Gamma}}_n = \sum_{i=1}^p \widehat{\lambda}_i \widehat{\mathbf{q}}_i \widehat{\mathbf{q}}_i^\top,$$

where $\widehat{\lambda}_i$ is the i th largest eigenvalue of $\widehat{\mathbf{\Gamma}}_n$ and $\widehat{\mathbf{q}}_i$ is its corresponding eigenvector. The input idiosyncratic volatility matrix estimator is

$$\widetilde{\mathbf{\Gamma}}^s = (\widetilde{\Gamma}_{ij}^s)_{i,j=1,\dots,p} = \widehat{\mathbf{\Gamma}}_n - \sum_{i=1}^r \widehat{\lambda}_i \widehat{\mathbf{q}}_i \widehat{\mathbf{q}}_i^\top,$$

and we apply the following adaptive thresholding scheme to the above input:

$$\widehat{\Gamma}_{ij}^s = \begin{cases} \widetilde{\Gamma}_{ij}^s \vee 0, & \text{if } i = j \\ s_{ij}(\widetilde{\Gamma}_{ij}^s) \mathbf{1}(|\widetilde{\Gamma}_{ij}^s| \geq \varpi_{ij}), & \text{if } i \neq j \end{cases} \quad \text{and} \quad \widehat{\mathbf{\Gamma}}^s = (\widehat{\Gamma}_{ij}^s)_{1 \leq i,j \leq p}, \quad (4.3)$$

where the thresholding function $s_{ij}(\cdot)$ satisfies $|s_{ij}(x) - x| \leq \varpi_{ij}$, and takes the thresholding level $\varpi_{ij} = \varpi_{m,n} \sqrt{(\widetilde{\Gamma}_{ii}^s \vee 0)(\widetilde{\Gamma}_{jj}^s \vee 0)}$ that is based on the correlation structure. The thresholding function includes interesting examples such as hard thresholding and soft thresholding functions.

4.4 Parameter estimation

If the latent factor process $\mathbf{f}(t)$ can be identified and estimated consistently, we can easily apply the parameter estimation procedure developed in Section 3.2. As discussed in Section 4.2, we impose some structures on the factor loading matrix \mathbf{U} so that it is estimable, which is the minimum requirement for investigating the latent factor model. See Aït-Sahalia and Xiu (2017); Fan et al. (2013); Kim et al. (2018); Kim and Fan (2019); Kim et al. (2020) for more details. With a consistent estimator $\hat{\mathbf{U}}$, we now develop an estimation procedure for the model parameters in the high-dimensional set-up, where the number of assets are allowed to diverge, as the number of observations diverges. To implement the procedure developed in Section 3.2, we first need to estimate the open-to-close factor volatility matrices and the close-to-open factor returns as follows:

$$RV_k^* = p^{-2} \hat{\mathbf{U}}^\top \hat{\mathbf{\Gamma}}_k^H \hat{\mathbf{U}} \quad \text{and} \quad \mathbf{r}_k^*(\boldsymbol{\mu}) = p^{-1} \hat{\mathbf{U}}^\top [\mathbf{X}(k) - \mathbf{X}(k-1+\tau)] - (1-\tau)\boldsymbol{\mu}.$$

The conditional volatilities are

$$\begin{aligned} \hat{\mathbf{h}}_n^{*H}(\boldsymbol{\theta}) &= \text{vec}(\boldsymbol{\omega}_H^g) + \mathbf{R}_H^g \hat{\mathbf{h}}_{n-1}^{*H}(\boldsymbol{\theta}) + \frac{\mathbf{A}_H^g}{\tau} \text{vec}(RV_{n-1}^*) + \frac{\mathbf{B}_H^g}{1-\tau} \text{vec}(\mathbf{r}_{n-1}^*(\boldsymbol{\mu}) \mathbf{r}_{n-1}^{*\top}(\boldsymbol{\mu})), \\ \hat{\mathbf{h}}_n^{*L}(\boldsymbol{\theta}) &= \text{vec}(\boldsymbol{\omega}_L^g) + \mathbf{R}_L^g \hat{\mathbf{h}}_{n-1}^{*L}(\boldsymbol{\theta}) + \frac{\mathbf{A}_L^g}{\tau} \text{vec}(RV_n^*) + \frac{\mathbf{B}_L^g}{1-\tau} \text{vec}(\mathbf{r}_{n-1}^*(\boldsymbol{\mu}) \mathbf{r}_{n-1}^{*\top}(\boldsymbol{\mu})). \end{aligned}$$

Then, the weighted square loss function is

$$\begin{aligned} \hat{L}_{n,m}^*(\boldsymbol{\theta}) &= \frac{1}{2n} \sum_{k=1}^n \left[\left\{ \text{vech}(RV_k^*) - \tau \hat{\mathbf{h}}_{h,k}^{*H}(\boldsymbol{\theta}) \right\}^\top \hat{\mathbf{V}}_H^{-1} \left\{ \text{vech}(RV_k^*) - \tau \hat{\mathbf{h}}_{h,k}^{*H}(\boldsymbol{\theta}) \right\} \right. \\ &\quad \left. + \left\{ \mathbf{r}_{h,k}^{*2}(\boldsymbol{\mu}) - (1-\tau) \hat{\mathbf{h}}_{h,k}^{*L}(\boldsymbol{\theta}) \right\}^\top \hat{\mathbf{V}}_L^{-1} \left\{ \mathbf{r}_{h,k}^{*2}(\boldsymbol{\mu}) - (1-\tau) \hat{\mathbf{h}}_{h,k}^{*L}(\boldsymbol{\theta}) \right\} \right], \end{aligned}$$

where $\hat{\mathbf{h}}_{h,n}^{*H}(\boldsymbol{\theta}) = \text{vech}\left(\text{vec}^{-1}\left(\hat{\mathbf{h}}_n^{*H}(\boldsymbol{\theta})\right)\right)$, $\hat{\mathbf{h}}_{h,n}^{*L}(\boldsymbol{\theta}) = \text{vech}\left(\text{vec}^{-1}\left(\hat{\mathbf{h}}_n^{*L}(\boldsymbol{\theta})\right)\right)$, and $\mathbf{r}_{h,k}^{*2}(\boldsymbol{\mu}) = \text{vech}\left(\mathbf{r}_{n-1}^*(\boldsymbol{\mu}) \mathbf{r}_{n-1}^{*\top}(\boldsymbol{\mu})\right)$. We estimate the true parameter $\boldsymbol{\theta}_0$ by minimizing $\hat{L}_{n,m}^*(\boldsymbol{\theta})$, that is,

$$\hat{\boldsymbol{\theta}}^* = \arg \min_{\boldsymbol{\theta} \in \Theta} \hat{L}_{n,m}^*(\boldsymbol{\theta}), \quad (4.4)$$

where Θ is the parameter space of θ . We choose the weight matrices $\widehat{\mathbf{V}}_H$ and $\widehat{\mathbf{V}}_L$ as discussed in Section 3.3.

To investigate the asymptotic behavior of $\widehat{\theta}^*$, we need the following technical conditions.

Assumption 4.1.

- (a) *There exists a factor loading matrix estimator $\widehat{\mathbf{U}} = (\widehat{U}_{ij})_{i=1,\dots,p,j=1,\dots,r}$ such that, for some $b \geq 4$,*

$$\max_{1 \leq i \leq r} \mathbb{E} \left(\|p^{-1/2} \widehat{\mathbf{U}}_i - p^{-1/2} \text{sign}(\widehat{\mathbf{U}}_i^\top \mathbf{U}_i) \mathbf{U}_i\|_F^b \right) \leq C \nu_{m,n}^b,$$

where \mathbf{U}_i and $\widehat{\mathbf{U}}_i$ are the i th column of \mathbf{U} and $\widehat{\mathbf{U}}$, respectively, and $\nu_{m,n} = o(1)$;

- (b) $U_{ij} = O(1)$ and $\mathbf{U}^\top \mathbf{U} = p \mathbf{I}_r$;

- (c) $\pi(p)/p = o(1)$.

Remark 4.1. When $p^{-1/2} \mathbf{U}$ is the eigenmatrix of the factor volatility matrix, Theorem 3.1 from Kim and Fan (2019) shows that $\nu_{m,n}$ is $m^{-1/4} + n^{-1/2} + \pi(p)/p$. If we assume that the factor loading matrix is known, such as the GICS membership matrix, $\nu_{m,n}$ will be zero. When the membership matrix is unknown and we provide its estimator, the convergence rate $\nu_{m,n}$ will be the corresponding convergence rate of the estimator.

The following theorem establishes the asymptotic results for the proposed QMLE $\widehat{\theta}^*$.

Theorem 4.1. *Under Assumption 3.1(a)–(d) and Assumption 4.1, we have*

$$\left\| \widehat{\theta}^* - \theta_0 \right\|_{\max} = O_p \left(m^{-1/4} + n^{-1/2} + \nu_{m,n} + (\pi(p)/p)^{1/2} \right).$$

Remark 4.2. Theorem 4.1 shows that the proposed WLSE $\widehat{\theta}^*$ has the convergence rate $m^{-1/4} + n^{-1/2} + \nu_{m,n} + (\pi(p)/p)^{1/2}$. The term $m^{-1/4}$ is coming from estimating the integrated volatility matrix $\mathbf{\Gamma}_k$ non-parametrically, which is known as the optimal rate, given the presence of the market microstructure noises. The term $n^{-1/2}$ is the usual convergence rate of low-frequency analysis. The terms $\nu_{m,n}$ and $(\pi(p)/p)^{1/2}$ are the cost to handle the

large volatility matrix. Specifically, the term $\nu_{m,n}$ is the cost to estimate the latent factor loading matrix \mathbf{U} . Since we employ the high-dimensional latent factor process, we have the extra term $(\pi(p)/p)^{1/2}$ for identifying the factor process.

4.5 Large volatility matrix prediction

In this section, we demonstrate how to predict future large volatility matrices and investigate the asymptotic behaviors of the proposed method. Recall that the daily integrated volatility matrix can be decomposed into the factor and idiosyncratic volatility matrices. Let the forecast origin be n , and we are interested in constructing an estimator for

$$\mathbb{E}(\mathbf{\Gamma}_{n+1}|\mathcal{F}_n) = \mathbf{U}\mathbf{H}_{n+1}(\boldsymbol{\theta}_0)\mathbf{U}^\top + \mathbb{E}(\mathbf{\Gamma}_{n+1}^s|\mathcal{F}_n) \quad \text{a.s.}$$

For the latent factor volatility matrix $\boldsymbol{\Psi}_{n+1}$, the MOGI model structure produces the following iterative relationship

$$\begin{aligned} \mathbf{h}_{n+1}(\boldsymbol{\theta}_0) &= \mathbb{E}(\text{vec}(\boldsymbol{\Psi}_{n+1})|\mathcal{F}_n) \\ &= \text{vec}(\boldsymbol{\omega}_0^g) + \mathbf{R}_0^g \mathbf{h}_n^H(\boldsymbol{\theta}_0) + \frac{\mathbf{A}_0^g}{\tau} \int_{n-1}^{\tau+n-1} \text{vec}(\boldsymbol{\sigma}_t^\top \boldsymbol{\sigma}_t) dt + \frac{\mathbf{B}_0^g}{1-\tau} \text{vec}(\mathbf{r}_n \mathbf{r}_n^\top), \end{aligned}$$

where $\boldsymbol{\omega}_0^g$, \mathbf{R}_0^g , \mathbf{A}_0^g , and \mathbf{B}_0^g are defined in Theorem 2.1, and $\text{vec}(\mathbf{H}_{n+1}(\boldsymbol{\theta}_0)) = \mathbf{h}_{n+1}(\boldsymbol{\theta}_0)$. With the WLSE $\hat{\boldsymbol{\theta}}^*$ defined in (4.4), we estimate the latent factor volatility matrix $\mathbf{H}_{n+1}(\boldsymbol{\theta}_0)$ by

$$\hat{\mathbf{H}}_{n+1}(\hat{\boldsymbol{\theta}}^*) = \text{vec}^{-1}(\hat{\mathbf{h}}_{n+1}(\hat{\boldsymbol{\theta}}^*)), \quad (4.5)$$

where

$$\hat{\mathbf{h}}_{n+1}(\hat{\boldsymbol{\theta}}^*) = \text{vec}(\boldsymbol{\omega}^g) + \mathbf{R}^g \hat{\mathbf{h}}_n(\hat{\boldsymbol{\theta}}^*) + \frac{\mathbf{A}^g}{\tau} \text{vec}(RV_n^*) + \frac{\mathbf{B}^g}{1-\tau} \text{vec}(\mathbf{r}_n^*(\boldsymbol{\mu}) \mathbf{r}_n^{*\top}(\boldsymbol{\mu})).$$

On the other hand, we impose the constant assumption on the idiosyncratic volatility matrix, that is,

$$\mathbb{E}(\mathbf{\Gamma}_{n+1}^s|\mathcal{F}_n) = \mathbf{\Gamma}^s \quad \text{a.s.}$$

and estimate $\mathbf{\Gamma}^s$ using the POET procedure as discussed in Section 4.3. Combining the factor volatility matrix estimator in (4.5) and the idiosyncratic volatility matrix estimator in (4.3), we estimate the conditional expectation of the future large volatility matrix $E(\mathbf{\Gamma}_{n+1}|\mathcal{F}_n)$ by

$$\tilde{\mathbf{\Gamma}}_{n+1} = \hat{\mathbf{U}}\hat{\mathbf{H}}_{n+1}(\hat{\boldsymbol{\theta}}^*)\hat{\mathbf{U}}^\top + \hat{\mathbf{\Gamma}}^s.$$

Under some conditions, Fan and Kim (2018) showed that the idiosyncratic volatility matrix estimator is consistent in the sense of the matrix spectral norm, and they established the asymptotic theorems for the estimator of the future large volatility matrix under the factor GARCH-Itô model. We employ their results to investigate the asymptotic behaviors of $\tilde{\mathbf{\Gamma}}_{n+1}$ and require the following technical conditions.

Assumption 4.2.

- (a) *There exists some fixed positive constant c_1 such that $\lambda_{n,1}/D_\lambda \leq c_1$ a.s., where $\lambda_{n,i}$ is the i th largest eigenvalue of $\mathbf{U}\Psi_n\mathbf{U}^\top$ and $D_\lambda = \min\{\lambda_{j,i} - \lambda_{j,i+1} : i = 1, \dots, r, j = 1, \dots, n\}$, and the smallest eigenvalue of $\mathbf{\Gamma}_n^s$ stays away from zero;*
- (b) *For some fixed constant c_2 , we have*

$$\frac{p}{r} \max_{1 \leq i \leq p} \sum_{j=1}^r q_{ij}^2 \leq c_2 \text{ a.s.},$$

where $\mathbf{q}_j = (q_{1j}, \dots, q_{pj})^\top$ is the j th eigenvector of $\mathbf{U}\Psi_n\mathbf{U}^\top$;

- (c) *The input volatility matrix $\hat{\mathbf{\Gamma}}_n$ satisfies*

$$\Pr \left\{ \max_{1 \leq i, j \leq p} |\hat{\Gamma}_{n,ij} - \bar{\Gamma}_{n,ij}| \geq C \sqrt{\frac{\log p}{m^{1/2}n + m}} \right\} \leq p^{-1}; \quad (4.6)$$

- (d) $\pi(p)/\sqrt{p} + \sqrt{\log p/(m^{1/2}n + m)} = o(1)$.

Remark 4.3. Assumption 4.2(a)–(b) are called the pervasive condition and incoherence condition, respectively, which are widely employed to investigate the behavior of the low-rank

matrix inferences (Candès et al., 2011; Fan et al., 2018). For example, the pervasive condition helps to identify the latent factor volatility matrix as the eigenvalues diverge with the order p while the eigenvalues of the idiosyncratic volatility matrix are bounded. On the other hand, the incoherence condition makes it possible to establish the element-wise convergence rate of the factor volatility matrix. The sub-Gaussian concentration inequality condition Assumption 4.2 (c) is required to investigate the high-dimensional statistics. Under some regularity conditions, the realized volatility estimators can obtain this bound (Fan and Kim, 2018; Tao et al., 2013).

Theorem 4.2. *Under the assumptions of Theorem 4.1, the sparsity condition (4.1) and Assumption 4.2 are met. Take the thresholding level to be $\varpi_{m,n} = C_\varpi b_{m,n}$ for some large fixed constant C_ϖ , where $b_{m,n} = \pi(p)/p + \sqrt{\log(p \vee m)/(nm^{1/2} + m)}$. Then we have*

$$\|\widehat{\mathbf{\Gamma}}^s - \mathbf{\Gamma}^s\|_{\max} = O_p(b_{m,n}), \quad (4.7)$$

$$\|\widehat{\mathbf{\Gamma}}^s - \mathbf{\Gamma}^s\|_2 = O_p(\pi(p)b_{m,n}^{1-\delta}), \quad (4.8)$$

$$\begin{aligned} \|\widetilde{\mathbf{\Gamma}}_{n+1} - \mathbb{E}(\mathbf{\Gamma}_{n+1}|\mathcal{F}_n)\|_{\mathbf{\Gamma}^*} &= O_p\left(m^{-1/4} + n^{-1/2} + \nu_{m,n} + \frac{\pi(p)}{p^{1/2}} \right. \\ &\quad \left. + p^{1/2}(m^{-1/2} + n^{-1} + \nu_{m,n}^2) + \pi(p)b_{m,n}^{1-\delta}\right), \end{aligned} \quad (4.9)$$

where the relative Frobenius norm is defined as $\|\mathbf{M}\|_{\mathbf{\Gamma}^*}^2 = p^{-1}\|\mathbf{\Gamma}^{*-1/2}\mathbf{M}\mathbf{\Gamma}^{*-1/2}\|_F^2$ where $\mathbf{\Gamma}^* = \mathbb{E}(\mathbf{\Gamma}_{n+1}|\mathcal{F}_n)$.

Remark 4.4. Theorem 4.2 shows that the estimator of the future volatility matrix $\widetilde{\mathbf{\Gamma}}_{n+1}$ has the convergence rate $m^{-1/4} + n^{-1/2} + \nu_{m,n} + \frac{\pi(p)}{p^{1/2}} + p^{1/2}(m^{-1/2} + n^{-1} + \nu_{m,n}^2) + \pi(p)b_{m,n}^{1-\delta}$ under the relative Frobenius norm. When the factor loading matrix \mathbf{U} is related to the eigenmatrix (Kim and Fan, 2019), $\nu_{m,n}$ will be $m^{-1/4} + \pi(p)/p$. Then $\widetilde{\mathbf{\Gamma}}_{n+1}$ will be consistent, as long as $p = o(m)$.

5 Simulation study

In this section, we show that the proposed methodology has good finite sample performance in estimation and prediction via a simulation study. Let p be the total number of assets, n

be the total number of low-frequency periods, and m be the total number of high-frequency returns during each low-frequency period. Let r be the number of common market factors in the high-dimensional set-up. The number of daily trading hours in the US market is 6.5, hence we choose $\tau = 6.5/24$.

5.1 A finite number of assets

We first investigated the low-dimensional case where $p = 3$ and generated the log prices $\mathbf{X}(t) = (X_1(t), \dots, X_p(t))^\top$ at discrete time points $t_{k,\ell} = k - 1 + \ell/(m/\tau)$, where $k = 1, \dots, n$ and $\ell = 1, \dots, m/\tau$ based on the multivariate Itô diffusion process. For the parameter matrices in the instantaneous volatility process defined in (2.1), we took the following values:

$$\begin{aligned} \text{vech}(\boldsymbol{\omega}_{H1}) &= (0.04, 0, 0, 0.04, 0, 0.08), & \text{vech}(\boldsymbol{\omega}_{H2}) &= (0.004, 0, 0, 0.004, 0, 0.004), \\ \text{vech}(\boldsymbol{\omega}_{L1}) &= (0.004, 0, 0, 0.016, 0, 0.012), & \text{vech}(\boldsymbol{\omega}_{L2}) &= (0.0012, 0, 0, 0.004, 0, 0.004), \\ \text{vech}(\boldsymbol{\gamma}_H) &= (0.4, 0.1, 0, 0.5, 0, 0.3), & \text{vech}(\boldsymbol{\gamma}_L) &= (0.7, 0, 0, 0.6, 0, 0.8), \\ \text{vech}(\boldsymbol{\beta}_H) &= (0.8, -0.1, 0.1, 0.7, -0.1, 0.6), & \text{vech}(\boldsymbol{\beta}_L) &= (0.2, 0, 0, 0.3, -0.1, 0.2), \\ \text{vech}(\boldsymbol{\nu}) &= (0, 0.08, 0.08, 0, 0.08, 0), & \boldsymbol{\mu} &= 0. \end{aligned}$$

It follows that the true parameter $\boldsymbol{\theta}_0$ is

$$\begin{aligned} \boldsymbol{\theta}_0 &= (\text{vech}(\boldsymbol{\omega}_{H0}^g), \text{vech}(\boldsymbol{\omega}_{L0}^g), \text{vech}(\boldsymbol{\gamma}_{H0}), \text{vech}(\boldsymbol{\gamma}_{L0}), \text{vech}(\boldsymbol{\beta}_{H0}), \text{vech}(\boldsymbol{\beta}_{L0}), \boldsymbol{\mu}_0) \\ &= (0.0044, 0.0022, 0.0014, 0.0070, 0.0010, 0.0067, 0.0018, 0.0011, -0.0000, \\ &\quad 0.0044, -0.0001, 0.0031, 0.4, 0.1, 0, 0.5, 0, 0.3, 0.7, 0, 0, 0.6, 0, 0.8, 0.8, \\ &\quad -0.1, 0.1, 0.7, -0.1, 0.6, 0.2, 0, 0, 0.3, -0.1, 0.2, 0, 0, 0). \end{aligned}$$

Initial values for simulation were chosen to be

$$\begin{aligned} \text{vech}(\boldsymbol{\Sigma}_0) &= \text{vech}(\boldsymbol{\omega}^g) = c(0.0039, 0.0018, 0.0008, 0.0066, 0.0002, 0.0054) \quad \text{and} \\ \mathbf{X}_0 &= (10, 10, 10)^\top. \end{aligned}$$

Market microstructure noises were modeled by i.i.d. $N(0, 0.001^2)$ random variables and were added to the simulated log prices $X_i(t_{k,\ell})$ between market open and close to generate high-frequency data $Y_i(t_{k,\ell})$, $\ell = 1, \dots, m-1$.

We employed the PRVM estimator (Christensen et al., 2010; Jacod et al., 2009) to estimate the daily integrated volatility matrix with open-to-close high-frequency data and denoted the corresponding estimators by RV_k , $k = 1, \dots, n$. The close-to-open low-frequency log returns $\mathbf{X}(k) - \mathbf{X}(k-1+\tau) - (1-\tau)\hat{\boldsymbol{\mu}}$ were computed. Parameter estimates were obtained by minimizing the proposed weighted square loss function $\hat{L}_{n,m}(\boldsymbol{\theta})$. We took $n = 125, 250, 500$ and $m = 390, 780, 2340$. We repeated the simulation 500 times.

Figure 1 depicts the mean matrix spectral norms, Frobenius norms, and max norms of $\hat{\boldsymbol{\omega}}_H^g - \boldsymbol{\omega}_{H0}^g$, $\hat{\boldsymbol{\omega}}_L^g - \boldsymbol{\omega}_{L0}^g$, $\hat{\boldsymbol{\gamma}}_H - \boldsymbol{\gamma}_{H0}$, $\hat{\boldsymbol{\gamma}}_L - \boldsymbol{\gamma}_{L0}$, $\hat{\boldsymbol{\beta}}_H - \boldsymbol{\beta}_{H0}$, and $\hat{\boldsymbol{\beta}}_L - \boldsymbol{\beta}_{L0}$ of the proposed MOGI estimator with $n = 125, 250, 500$ and $m = 390, 780, 2340$. From Figure 1, we find that the mean matrix estimation errors decrease as the number of high-frequency observations or low-frequency observations increases.

We studied the prediction performance of the proposed methodology. Specifically, we utilized the model structure to estimate the conditional future daily integrated volatility matrix $E(\int_n^{n+1} \boldsymbol{\Sigma}_t dt | \mathcal{F}_n)$ by $\hat{\mathbf{H}}_{n+1}(\hat{\boldsymbol{\theta}}) = \text{vec}^{-1}(\hat{\mathbf{h}}_{n+1}(\hat{\boldsymbol{\theta}}))$. For each simulation, we computed the matrix estimation error for $\hat{\mathbf{H}}_{n+1}(\hat{\boldsymbol{\theta}}) - \mathbf{H}_{n+1}(\boldsymbol{\theta})$ in the spectral norm, Frobenius norm, max norm, and relative Frobenius norm. For comparisons, we consider the BEKK(1,1) model (BEKK) (Engle and Kroner, 1995) using low-frequency observations, which is the sequence of the open-to-open returns $\mathbf{X}(k) - \mathbf{X}(k-1)$, $k = 1, \dots, n$, a nonparametric estimator $RV_n + (\mathbf{X}(n) - \mathbf{X}(n-1+\tau))(\mathbf{X}(n) - \mathbf{X}(n-1+\tau))^\top$, where RV_n is estimated by the PRVM estimator using high-frequency observations (PRVM), and the scaled multivariate GARCH-Itô model (MGI), where the multivariate GARCH-Itô model is a particular type of the MOGI model that is able to estimate open-to-close volatility. The MGI model only considers open-to-close volatility. If we set parameters in the MOGI model as $\tau = 1$, $\boldsymbol{\gamma}_L = \mathbf{I}_p$, and $\boldsymbol{\beta}_L = \mathbf{0}$, then the MOGI model becomes the MGI model. Under the MGI model, the

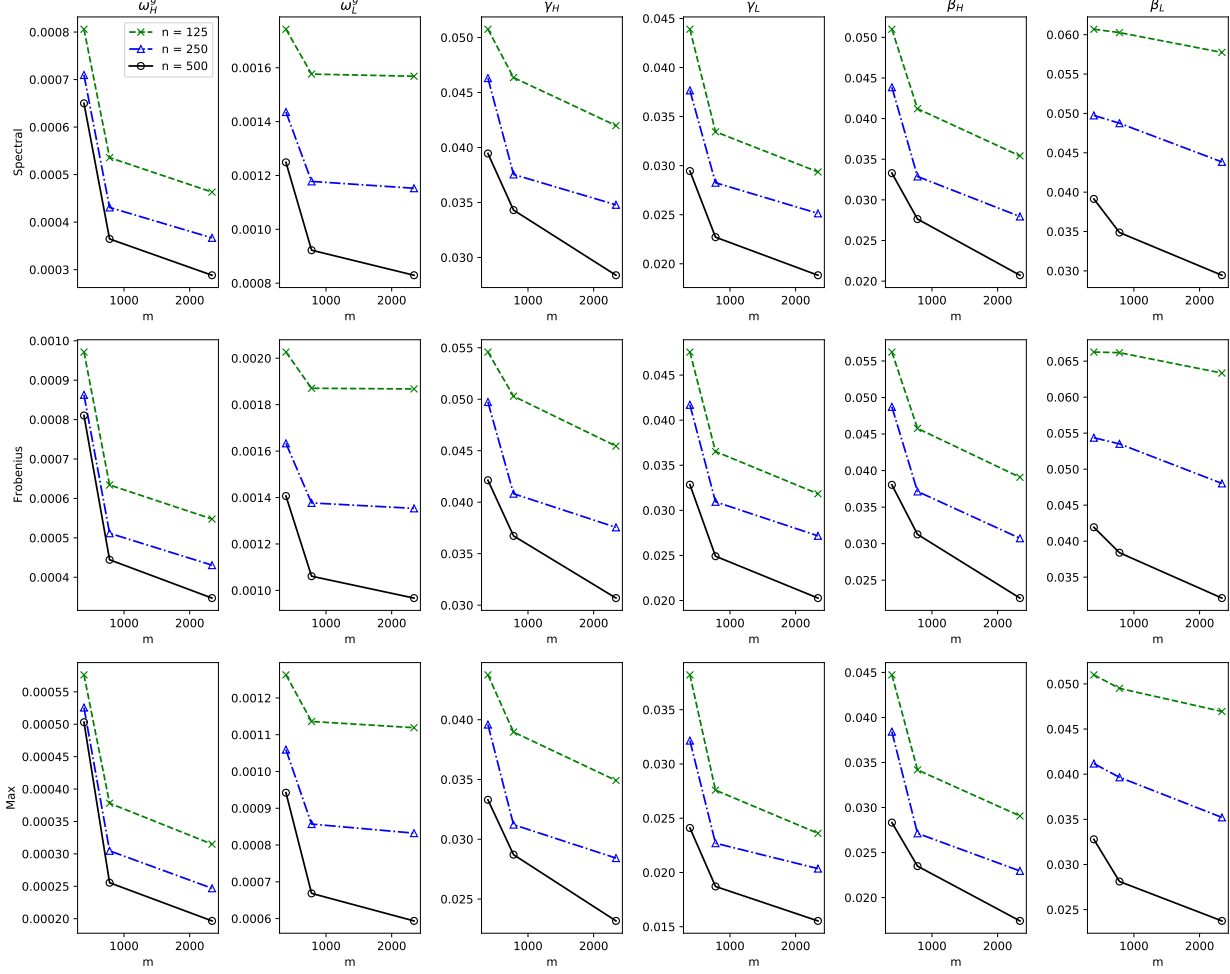


Figure 1: Mean matrix spectral norms, Frobenius norms, and max norms of $\hat{\omega}_H^g - \omega_{H0}^g$, $\hat{\omega}_L^g - \omega_{L0}^g$, $\hat{\gamma}_H - \gamma_{H0}$, $\hat{\gamma}_L - \gamma_{L0}$, $\hat{\beta}_H - \beta_{H0}$, and $\hat{\beta}_L - \beta_{L0}$ of the proposed MOGI estimator with $n = 125, 250, 500$ and $m = 390, 780, 2340$.

conditional open-to-close volatility can be estimated as follows:

$$\hat{\mathbf{h}}_{n+1}(\hat{\boldsymbol{\theta}}) = \text{vec}(\boldsymbol{\omega}) + \mathbf{R}^g \hat{\mathbf{h}}_n(\hat{\boldsymbol{\theta}}) + \mathbf{A}^g \text{vec}(RV_n),$$

where $\hat{\boldsymbol{\theta}} = (\text{vech}(\boldsymbol{\omega}), \text{vech}(\boldsymbol{\gamma}), \text{vech}(\boldsymbol{\beta}))$, $\mathbf{R} = \boldsymbol{\gamma} \otimes \boldsymbol{\gamma}$, $\mathbf{B} = \boldsymbol{\beta} \otimes \boldsymbol{\beta}$, $\boldsymbol{\varrho}_1 = \mathbf{B}^{-1}(e^{\mathbf{B}} - \mathbf{I}_{p^2})$, $\boldsymbol{\varrho}_2 = \mathbf{B}^{-2}(e^{\mathbf{B}} - \mathbf{I}_{p^2} - \mathbf{B})$, $\boldsymbol{\varrho}_3 = \mathbf{B}^{-3}(e^{\mathbf{B}} - \mathbf{I}_{p^2} - \mathbf{B} - \mathbf{B}^2/2)$, $\boldsymbol{\varrho} = 2\boldsymbol{\varrho}_3\mathbf{R} + \boldsymbol{\varrho}_1 - \boldsymbol{\varrho}_2$, $\mathbf{R}^g = \boldsymbol{\varrho}\mathbf{R}\boldsymbol{\varrho}^{-1}$, and $\mathbf{A}^g = \boldsymbol{\varrho}\mathbf{B}$. The model parameter can be estimated by the least squares estimators as

follows:

$$\hat{\boldsymbol{\theta}} = \arg \min_{\boldsymbol{\theta}} \frac{1}{2n} \sum_{k=1}^n \{ \text{vech}(RV_k) - \hat{\mathbf{h}}_k(\boldsymbol{\theta}) \}^\top \{ \text{vech}(RV_k) - \hat{\mathbf{h}}_k(\boldsymbol{\theta}) \}.$$

To match the estimated open-to-close volatility with the daily integrated volatility, one can scale up the estimated open-to-close volatility as $\Lambda \hat{\mathbf{h}}_{n+1} \Lambda$, where Λ is a diagonal matrix such that $\Lambda = \text{diag}(\sqrt{([\overline{RV}_n]_{11} + [\overline{OV}_n]_{11}) [\overline{RV}_n]_{11}^{-1}}, \dots, \sqrt{([\overline{RV}_n]_{pp} + [\overline{OV}_n]_{pp}) [\overline{RV}_n]_{pp}^{-1}})$, $\overline{RV}_n = \frac{1}{n} \sum_{k=1}^n RV_k$, $\overline{OV}_n = \frac{1}{n} \sum_{k=1}^n OV_k$, and $OV_k = \mathbf{r}_k \mathbf{r}_k^\top$.

Figure 2 depicts the mean matrix prediction errors in the spectral norms, Frobenius norms, max norms, and relative Frobenius norms for the conditional daily integrated volatility matrix $E(\int_n^{n+1} \boldsymbol{\Sigma}_t dt | \mathcal{F}_n)$ with the MOGI, MGI, BEKK, and PRVM estimators with $n = 125, 250, 500$ and $m = 390, 780, 2340$. From Figure 2, we observe that, as the number of high-frequency observations or low-frequency observations increases, the prediction performance of the MOGI model becomes better. The MOGI model presents better performance than the BEKK, PRVM, and MGI models.

5.2 A large number of assets

We now investigate the high-dimensional case for $p = 200$ and $r = 3$. For the instantaneous latent factor volatility process described by (2.1), we took the model parameters as follows:

$$\begin{aligned} \text{vech}(\boldsymbol{\omega}_{H1}) &= (0.06, 0, 0, 0.08, 0, 0.04), & \text{vech}(\boldsymbol{\omega}_{H2}) &= (0.004, 0, 0, 0.004, 0, 0.004), \\ \text{vech}(\boldsymbol{\omega}_{L1}) &= (0.024, 0, 0, 0.012, 0, 0.004), & \text{vech}(\boldsymbol{\omega}_{L2}) &= (0.006, 0, 0, 0.004, 0, 0.012), \\ \text{vech}(\boldsymbol{\gamma}_H) &= (0.5, 0, 0, 0.3, 0, 0.4), & \text{vech}(\boldsymbol{\gamma}_L) &= (0.6, 0, 0, 0.8, 0, 0.7) \\ \text{vech}(\boldsymbol{\beta}_H) &= (0.7, 0, 0, 0.6, 0, 0.8), & \text{vech}(\boldsymbol{\beta}_L) &= (0.3, 0, 0, 0.25, 0, 0.2) \\ \boldsymbol{\nu} &= \text{diag}(0.06, 0.04, 0.03), & \boldsymbol{\mu} &= 0. \end{aligned}$$

It follows that the true parameter $\boldsymbol{\theta}_0$ is

$$\begin{aligned} \boldsymbol{\theta}_0 &= (\text{vech}(\boldsymbol{\omega}_{H0}^g), \text{vech}(\boldsymbol{\omega}_{L0}^g), \text{vech}(\boldsymbol{\gamma}_{H0}), \text{vech}(\boldsymbol{\gamma}_{L0}), \text{vech}(\boldsymbol{\beta}_{H0}), \text{vech}(\boldsymbol{\beta}_{L0}), \boldsymbol{\mu}_0) \\ &= (0.0089, 0, 0, 0.0045, 0, 0.0018, 0.0075, 0, 0, 0.0031, 0, 0.0018, 0.5, 0, 0, 0.3, 0, 0.4, \\ &\quad 0.6, 0, 0, 0.8, 0, 0.7, 0.7, 0, 0, 0.6, 0, 0.8, 0.3, 0, 0, 0.25, 0, 0.2, 0, 0, 0). \end{aligned}$$

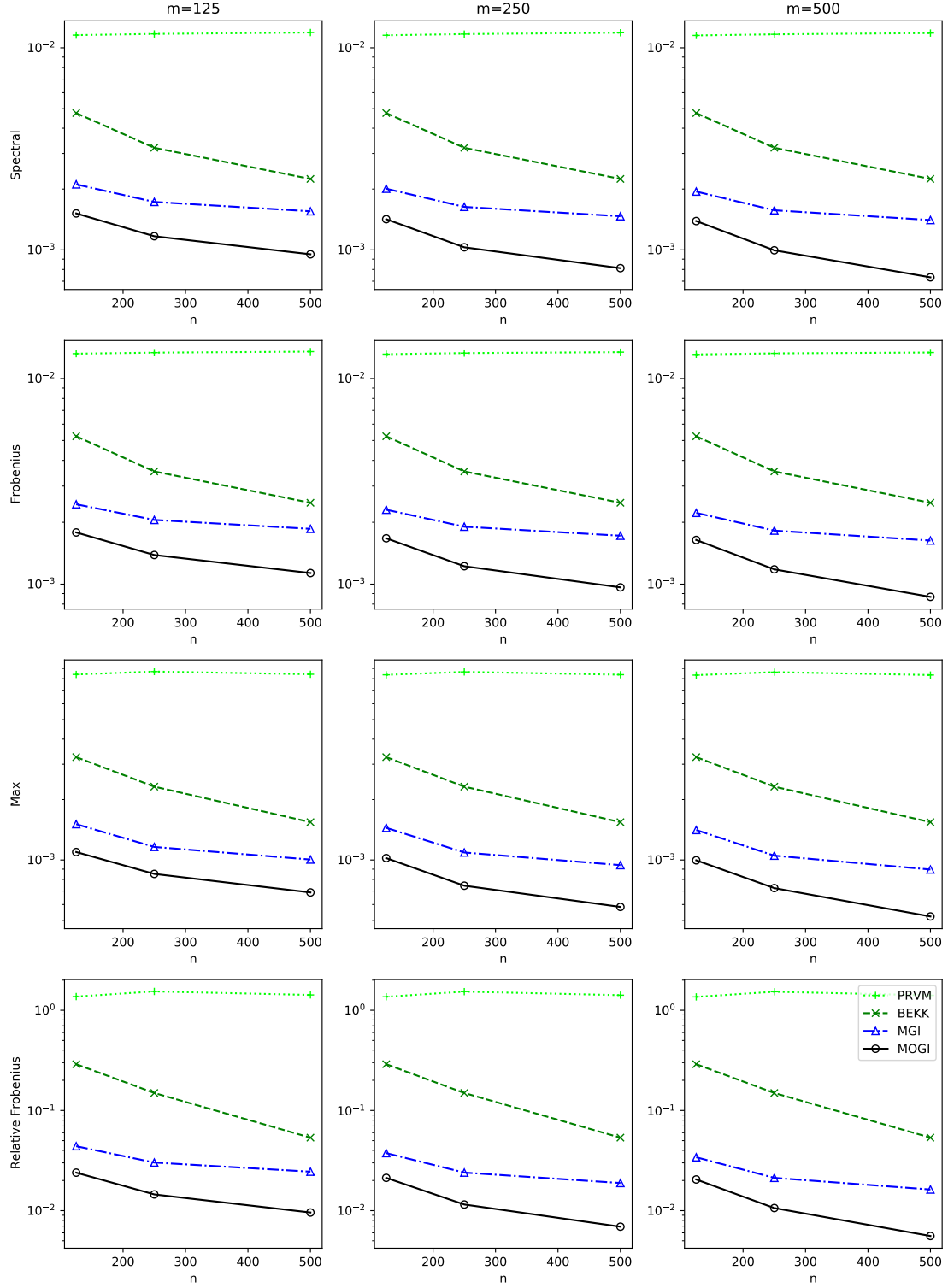


Figure 2: Mean matrix prediction errors in the spectral, Frobenius, max, and relative Frobenius norms for the conditional daily integrated volatility matrix $E(\int_n^{n+1} \Sigma_t dt | \mathcal{F}_n)$ calculated by the MOGI, MGI, BEKK, and PRVM estimators with $n = 125, 250, 500$ and $m = 390, 780, 2340$.

Initial values for simulation were chosen to be

$$\begin{aligned}\text{vech}(\boldsymbol{\Sigma}_0) &= \text{vech}(\boldsymbol{\omega}^g) = c(0.0100, 0, 0, 0.0044, 0, 0.0024), \\ \mathbf{f}(t) &= (10, 10, 10)^\top, \quad \mathbf{X}(t) = (10, \dots, 10)^\top.\end{aligned}$$

For the factor loading matrix \mathbf{U} , \mathbf{U}_1 takes values $\sqrt{2} \cos(2i\pi/p)$, $i = 1, \dots, p$, \mathbf{U}_2 entries share the same value 1, and \mathbf{U}_3 takes values $\sqrt{2} \sin(2i\pi/p)$, $i = 1, \dots, p$. Then the factor loading matrix retains the structure such that $\mathbf{U}^\top \mathbf{U} = p\mathbf{I}_r$, which is the condition required in Kim et al. (2020) for obtaining a consistent estimator of \mathbf{U} by using the eigenmatrix of the variance of all daily integrated volatility matrices. To generate the sparse idiosyncratic diffusion process in its daily integrated co-volatility $\boldsymbol{\Gamma}^s = (\Gamma_{ij}^s)_{1 \leq i, j \leq p}$, we took

$$\Gamma_{ij}^s = 0.5^{|i-j|} \sqrt{\Gamma_{ii}^s \Gamma_{jj}^s}$$

for the off-diagonal elements and $\Gamma_{ii}^s = 0.004$, $i = 1, \dots, p$, for the diagonal elements. Market microstructure noises were modeled by independent $N(0, 0.001^2)$. Given high-frequency data, the PRVM estimator was again adopted to obtain the daily large realized volatility matrix estimates $\hat{\boldsymbol{\Gamma}}_k^H$, $k = 1, \dots, n$. To estimate the factor loading matrix, we followed the procedure given in Kim et al. (2020). Specifically, let $\hat{\boldsymbol{\Gamma}}_n^H = \sum_{k=1}^n \hat{\boldsymbol{\Gamma}}_k^H / n$ be the sample mean and $\hat{\mathbf{S}}_n^H = \sum_{k=1}^n (\hat{\boldsymbol{\Gamma}}_k^H - \hat{\boldsymbol{\Gamma}}_n^H)^2 / (np)$ be the sample variance. We estimated $p^{-1/2}\mathbf{U}$ by the first r eigenvectors of $\hat{\mathbf{S}}_n^H$ and computed the low-rank factor volatility matrix estimates RV_k^* by $RV_k^* = p^{-2} \hat{\mathbf{U}}^\top \hat{\boldsymbol{\Gamma}}_k^H \hat{\mathbf{U}}$. The close-to-open factor returns $r_k^*(\mathbf{0}) = p^{-1} \hat{\mathbf{U}}^\top [\mathbf{X}(k) - \mathbf{X}(k-1 + \tau)]$ were obtained. Similar to the low-dimensional case, we employed $\tilde{\mathbf{V}}_H^*$, and $\tilde{\mathbf{V}}_L^*$ for the consistent estimators of \mathbf{V}_H^* , and \mathbf{V}_L^* , respectively. Parameter estimates were obtained by minimizing the proposed weighted square loss function $\hat{L}_{n,m}^*(\boldsymbol{\theta})$. We took $n = 125, 250, 500$ and $m = 390, 780, 2340$. We repeated the simulation 500 times.

Figure 3 depicts the mean matrix spectral norms, Frobenius norms, and max norms of $\hat{\boldsymbol{\omega}}_H^g - \boldsymbol{\omega}_{H0}^g$, $\hat{\boldsymbol{\omega}}_L^g - \boldsymbol{\omega}_{L0}^g$, $\hat{\boldsymbol{\gamma}}_H - \boldsymbol{\gamma}_{H0}$, $\hat{\boldsymbol{\gamma}}_L - \boldsymbol{\gamma}_{L0}$, $\hat{\boldsymbol{\beta}}_H - \boldsymbol{\beta}_{H0}$, and $\hat{\boldsymbol{\beta}}_L - \boldsymbol{\beta}_{L0}$ for the proposed MOGI estimator with $n = 125, 250, 500$ and $m = 390, 780, 2340$. From Figure 3, we find that the mean matrix estimation errors decrease as the number of high-frequency observations or

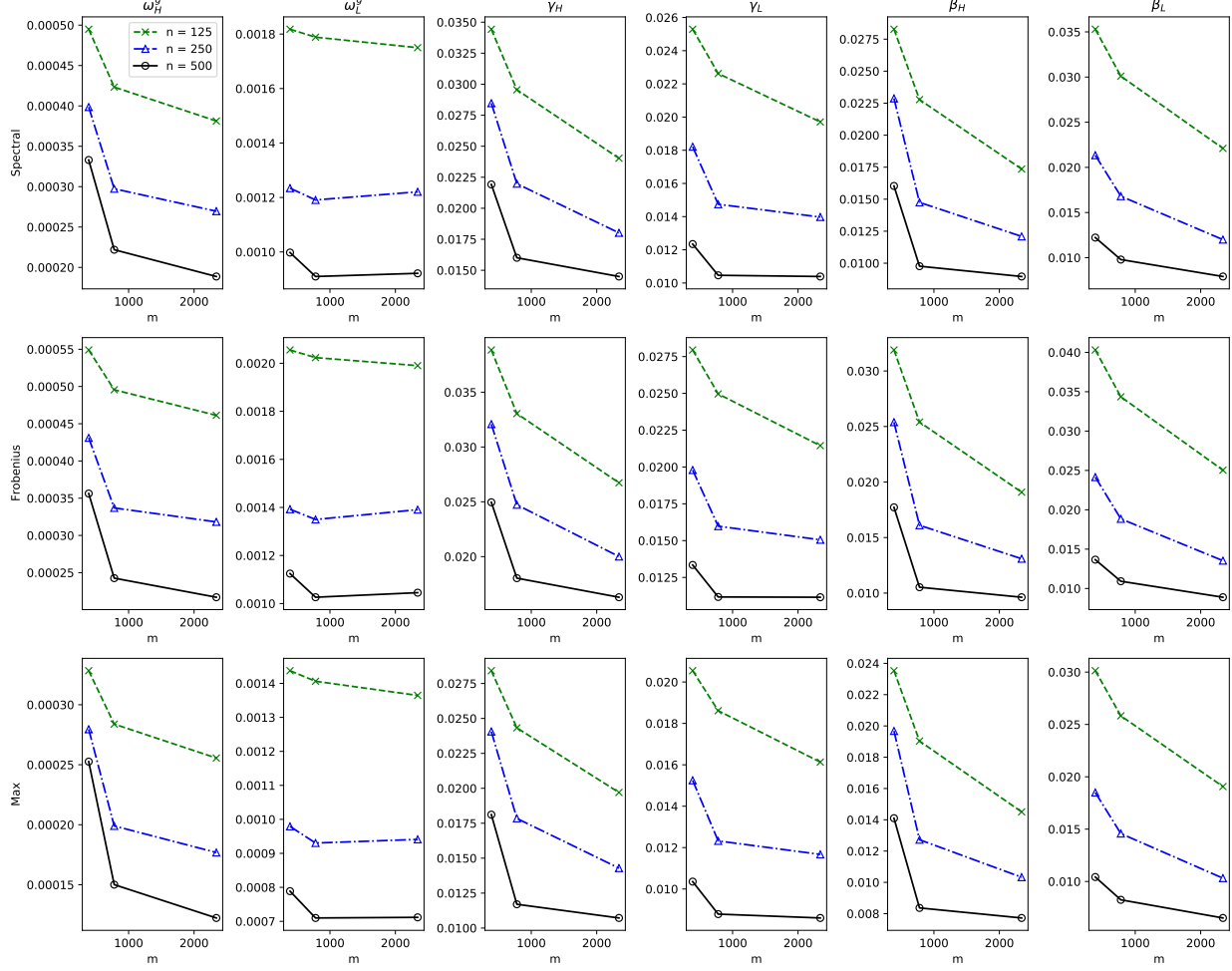


Figure 3: Mean matrix spectral norms, Frobenius norms, and max norms of $\hat{\omega}_H^g - \omega_{H0}^g$, $\hat{\omega}_L^g - \omega_{L0}^g$, $\hat{\gamma}_H - \gamma_{H0}$, $\hat{\gamma}_L - \gamma_{L0}$, $\hat{\beta}_H - \beta_{H0}$, and $\hat{\beta}_L - \beta_{L0}$ for the proposed MOGI estimator with $n = 125, 250, 500$ and $m = 390, 780, 2340$.

low-frequency observations increases, except for the $\hat{\omega}_L^g - \omega_{L0}^g$. We note that there is an unclear effect of increasing the number of high-frequency observations in the case of ω_L . This may be because the parameter ω_L affects the close-to-open periods, which provide the low-frequency observations, so high-frequency observations have relatively little effect on the estimation accuracy.

We as well studied the prediction performance of the proposed model and compared it with benchmarks. Specifically, we estimated the conditional large volatility matrix $E(\Gamma_{n+1}|\mathcal{F}_n)$ by $\tilde{\Gamma}_{n+1}$ and computed the matrix estimation errors for $\tilde{\Gamma}_{n+1} - E(\Gamma_{n+1}|\mathcal{F}_n)$ in spectral, Frobe-

nius, max, and relative Frobenius norm. To construct $\tilde{\mathbf{\Gamma}}_{n+1}$, we need to obtain the idiosyncratic volatility matrix estimator $\hat{\mathbf{\Gamma}}^s$, where we took $\sqrt{\log p/n} + \sqrt{1/p}$ to be the threshold. For comparisons, we considered the POET procedure proposed by Fan et al. (2013) and the MGI procedure, which is the same as that of the MOGI procedure based on the factor Itô diffusion process, except for the factor estimation that utilizes the scaled MGI estimator (see Section 5.1). We utilized $\hat{\mathbf{\Gamma}}_n^H + [\mathbf{X}(n) - \mathbf{X}(n-1)][\mathbf{X}(n) - \mathbf{X}(n-1)]^\top$ for the open-to-open covariance matrix in the POET procedure, and we took $\sqrt{2 \log p/m^{1/2}}$ to be the threshold for the thresholding step in the POET procedure.

Figure 4 draws the mean matrix prediction errors in the spectral norms, Frobenius norms, max norms, and relative Frobenius norms with the MOGI, MGI, and POET estimators with $n = 125, 250, 500$ and $m = 390, 780, 2340$. It is clear that the estimator based on the proposed MOGI method outperforms the benchmarks based on the POET and MGI procedures, except for the relative Frobenius norm. This may be because each eigenvalue in the relative Frobenius norm has a similar scale, and so the effect of the factor part is relatively small. Thus, the MOGI cannot present significant benefits in terms of the relative Frobenius norm. As the number of low- or high-frequency observations increases, the mean matrix prediction errors decrease, which supports the theoretical results derived in Section 4.

6 Empirical analysis

In this section, we apply the proposed MOGI model to real trading stock prices to examine the case for a large number of assets with $p = 200$ and focus on constrained portfolio allocation problems that are widely considered in financial applications. The data set consists of the minute-by-minute stock prices of companies that were traded on the New York Stock Exchange during the 504 trading days from January 2018 to December 2019. That is, in order to synchronize the observation time points, we used the previous tick (Zhang, 2011) scheme. The high-frequency trading data for the top 200 large volume stocks among the S&P 500 compositions was obtained from the Wharton Data Service (WRDS) system. The

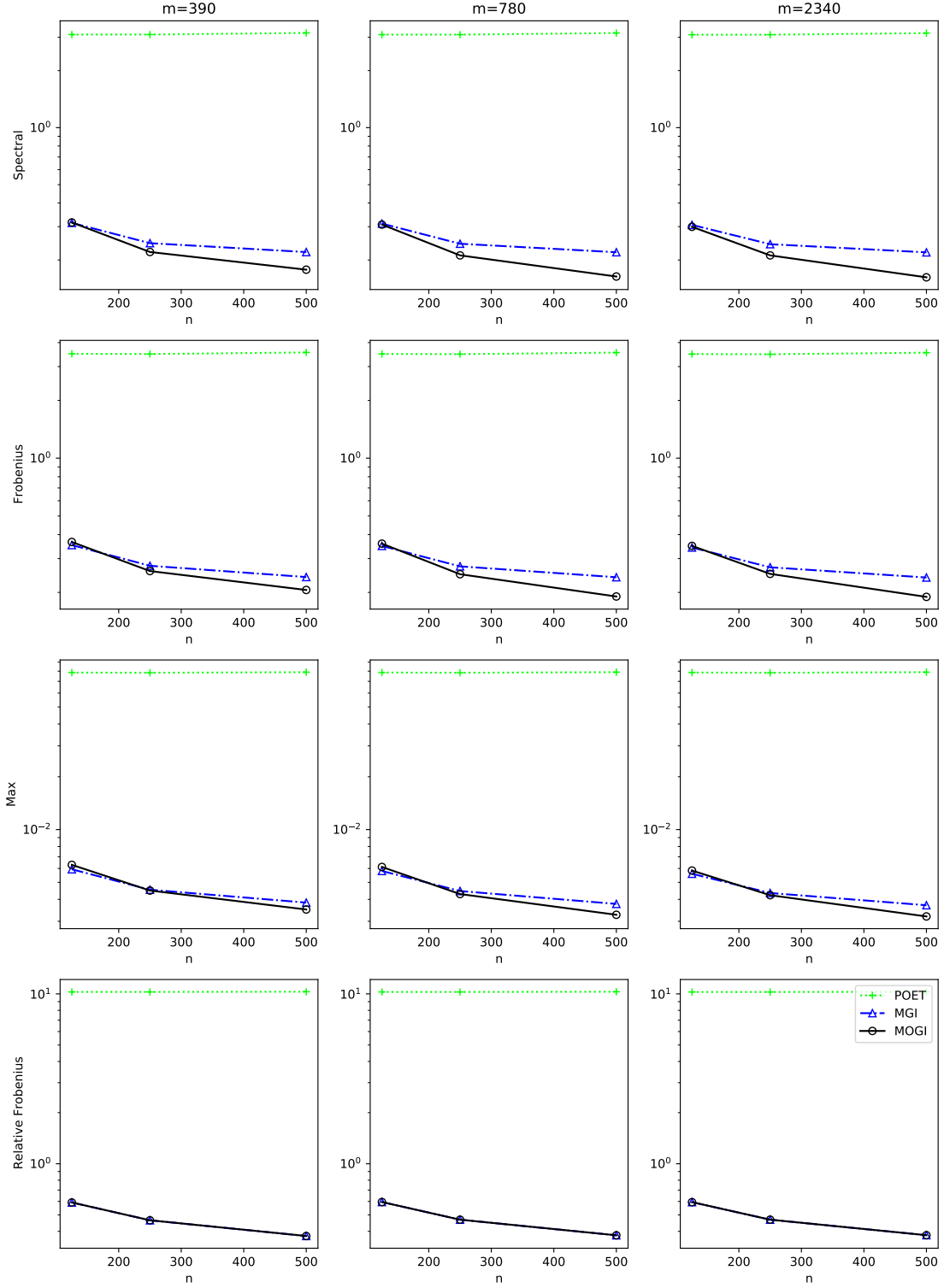


Figure 4: Mean matrix prediction errors in the spectral, Frobenius, max, and relative Frobenius norms for the conditional daily integrated volatility matrix $E(\Gamma_{n+1}|\mathcal{F}_n)$ with the MOGI, MGI, and POET estimators with $n = 125, 250, 500$ and $m = 390, 780, 2340$.

6.5 trading hours daily result in $\tau = 6.5/24$.

To forecast the one-day-ahead conditional volatility matrix, we employed the MOGI, MGI, and POET procedures explained in Section 5.2, where the only difference is a threshold level for the idiosyncratic volatility matrix estimators. Here, we used the global industry classification standard (GICS) for sectors and kept the volatilities within the same sector, but set others to be zero (Fan et al., 2016). We set the in-sample period as 126 days and used the rolling window scheme to estimate the one-day-ahead conditional volatility matrix for the MOGI and MGI models.

For the empirical case, the decomposition of daily variation into its continuous and jump components can help to explain the volatility dynamics due to the existence of price jumps (Aït-Sahalia et al., 2012; Andersen et al., 2007; Barndorff-Nielsen and Shephard, 2006; Corsi et al., 2010). Therefore, we employed the jump truncated PRVM estimator proposed by Aït-Sahalia and Xiu (2016) to obtain $\hat{\mathbf{\Gamma}}_k^H$, $k = 1, \dots, n$. Specifically, jump truncated PRVM were estimated as follows:

$$[\hat{\mathbf{\Gamma}}_k^H]_{ij} = \frac{1}{w\phi} \sum_{u=1}^{m-w+1} \left(\bar{X}_{k,u}^i \bar{X}_{k,u}^j - \frac{1}{2} \hat{X}_{k,u}^{ij} \right) \mathbb{1}(|\bar{X}_{k,u}^i| < v_k^i) \mathbb{1}(|\bar{X}_{k,u}^j| < v_k^j),$$

where $w = \lfloor m^{1/2} \rfloor$, $\phi = 1/12$, $g(x) = x \wedge (1 - x)$, $\Delta_u^k X_i = X_i(k - 1 + \tau u/m) - X_i(k - 1 + \tau(u - 1)/m)$, $\hat{X}_{k,u}^{ij} = \sum_{s=1}^w (g(\frac{s}{w}) - g(\frac{s-1}{w}))^2 \Delta_{u+s-1}^k X_i \Delta_{u+s-1}^k X_j$, $\bar{X}_{k,u}^i = \sum_{s=1}^{w-1} g(s/w) \Delta_{u+s}^k X_i$, and $v_k^i = 2.19 \sqrt{\sum_{u=1}^{m-w+1} (\bar{X}_{k,u}^i)^2 / (m - w + 1)}$ is a truncation parameter.

We then need to determine the number of market factors r so that the corresponding factor loading and factor volatility matrices can be identified and estimated. Figure 5 shows the scree plot for $\sum_{k=1}^n \hat{\lambda}_{k,1}/n, \sum_{k=1}^n \hat{\lambda}_{k,2}/n, \dots, \sum_{k=1}^n \hat{\lambda}_{k,200}/n$, where $\hat{\lambda}_{k,j}$ is the j th largest eigenvalue of $\hat{\mathbf{\Gamma}}_k^H$. From Figure 5, we find that possible candidates for the number of market factors r is 1,2,3,4. To further determine the rank r , we adopted the procedure as described in Aït-Sahalia and Xiu (2017),

$$\hat{r} = \arg \min_{1 \leq j \leq r_{\max}} \sum_{k=1}^{504} \left[p^{-1} \hat{\lambda}_{k,j} + j \times c_1 \left\{ \sqrt{\log p / m^{1/2}} + p^{-1} \log p \right\}^{c_2} \right] - 1,$$

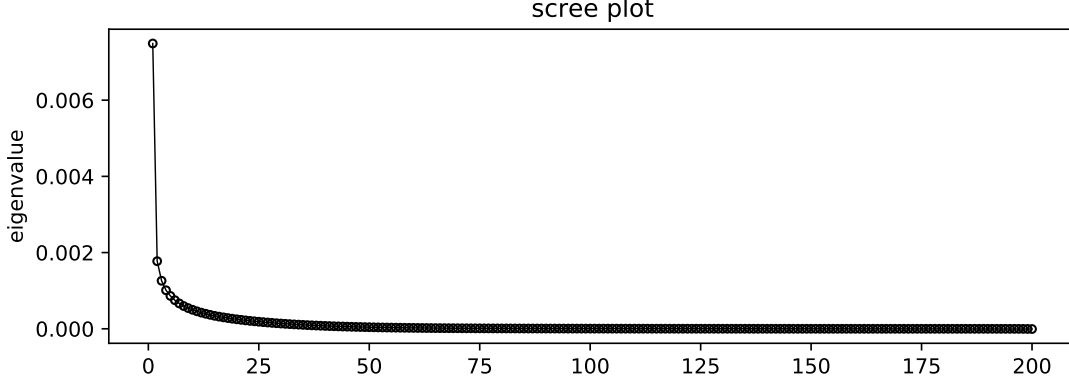


Figure 5: The scree plot of eigenvalues of the average of 504 daily PRVM estimators.

where $\hat{\lambda}_{k,j}$ is the j th largest eigenvalue of $\hat{\mathbf{\Gamma}}_k^H$. We studied the problem when $r_{\max} = 30$, $c_1 = 0.02\hat{\lambda}_{k,30}$, and $c_2 = 0.5$. The procedure chose $\hat{r} = 3$.

We revisited the constrained portfolio allocation problem (Fan et al., 2012). Given the estimated predictor $\tilde{\mathbf{\Gamma}}_k$ for a future large volatility matrix, we minimized the following portfolio risk function:

$$\min_{\mathbf{w}_k \text{ s.t. } \mathbf{w}_k^\top \mathbf{J} = 1 \text{ and } \|\mathbf{w}_k\|_1 \leq c_0} \mathbf{w}_k^\top \tilde{\mathbf{\Gamma}}_k \mathbf{w}_k,$$

where $\mathbf{J} = (1, \dots, 1)^\top \in \mathbb{R}^p$ and c_0 is the gross exposure constraint that ranges from 1 to 3. The portfolio associated with $\hat{\mathbf{w}}_k$ that minimizes the above function is the so-called optimal portfolio. For a given period with d days, we computed the out-of-sample portfolio risk for the optimal portfolios in the annualized form

$$R = \sqrt{\frac{252}{d} \sum_{k=1}^d \left(\sum_{i=1}^{39} r_{k,i}(\hat{\mathbf{w}}_k)^2 + r_k^{CO}(\hat{\mathbf{w}}_k)^2 \right)},$$

where $r_{k,i}(\hat{\mathbf{w}}_k) = \hat{\mathbf{w}}_k^\top (\mathbf{Y}(k-1 + \tau \frac{i}{39}) - \mathbf{Y}(k-1 + \tau \frac{i-1}{39}))$ is the 10-min portfolio log-return and $r_k^{CO}(\hat{\mathbf{w}}_k) = \hat{\mathbf{w}}_k^\top (\mathbf{Y}(k) - \mathbf{Y}(k-1 + \tau))$ is the close-to-open portfolio log-return of day k . We used three different out-of-sample periods—day 127 to day 252, day 253 to day 378, and day 379 to day 504—and the whole out-of-sample period.

Figure 6 plots the annualized out-of-sample portfolio risks with the MOGI, MGI, and

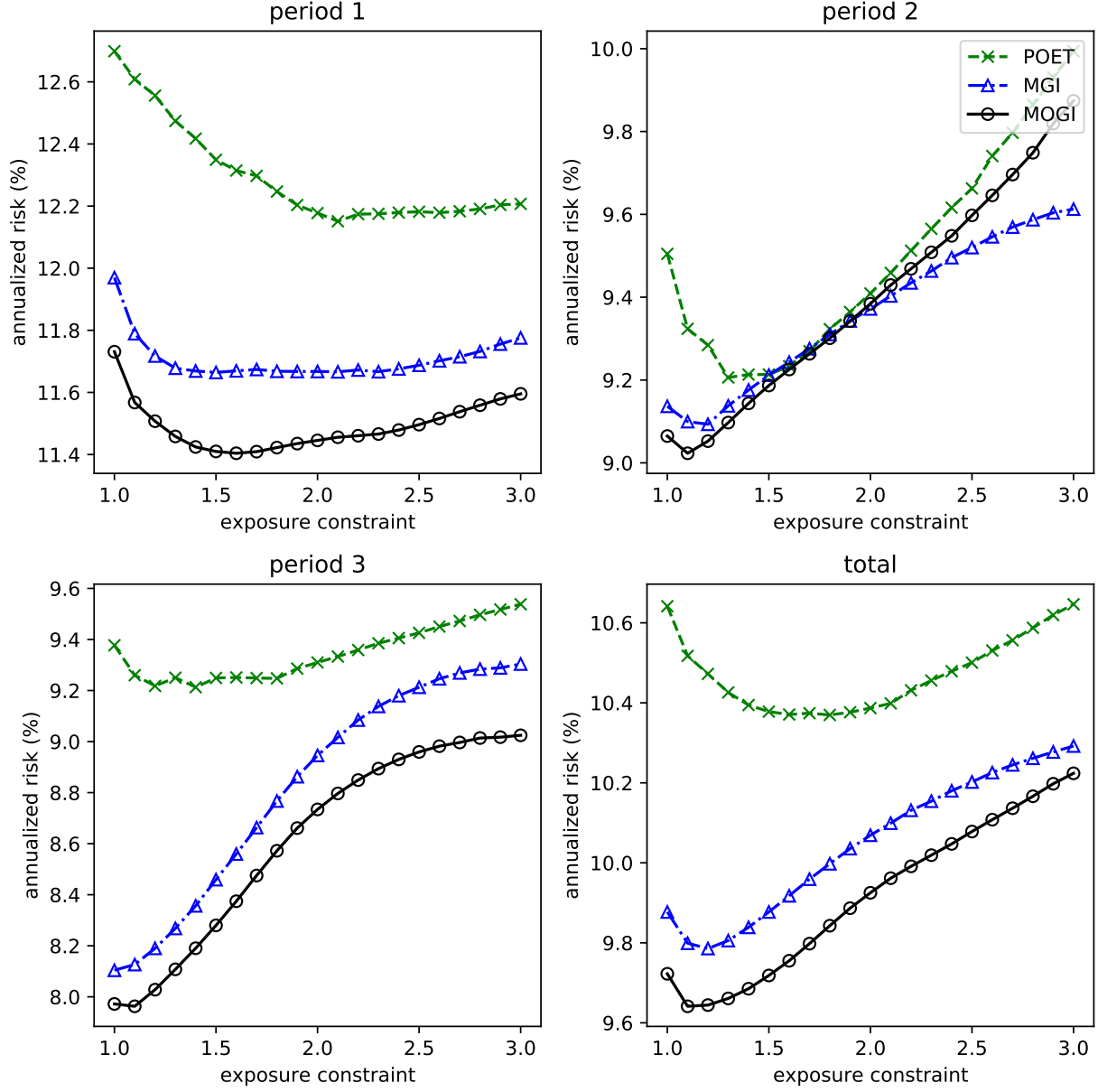


Figure 6: Annualized out-of-sample portfolio risks with the MOGI, MGI, and POET procedures against the gross exposure constraint c_0 for the three different periods and the whole period.

POET procedures for the three different periods—say, period 1, 2, and 3—and the whole period against the gross exposure constraint c_0 . From Figure 6, we find that the parametric models, the MOGI and MGI models, perform better than the POET method. It may be because the

factor has a time series dynamic structure. We note that the proposed MOGI model has the smallest portfolio risks among the methods, regardless of the periods. From these results, we may conjecture that the market factors have a time series dynamic structure and that incorporating close-to-open market factors helps to account for market dynamics.

7 Conclusion

In this paper, we propose the unified approach for describing the volatility matrix evolution by embedding the discrete-time multivariate GARCH model structure in the continuous-time Itô diffusion process. We first discuss the proposed method for the finite dimension. When the instantaneous volatility process is restricted to integer times, it retains the discrete-time multivariate GARCH model structure so that it can capture the rich dynamics in the volatility process. For the high-dimensional set-up, we model the stock price process by the factor Itô diffusion process so that the large volatility process can be decomposed into the factor and idiosyncratic volatility matrices. We embed the multivariate GARCH model structure in the instantaneous factor volatility process, and we assume that the idiosyncratic volatility process is a martingale. Model parameters in the MOGI model are estimated by minimizing the weighted loss function, and this estimating approach is proved to have good asymptotic behaviors. We demonstrate the validity of the proposed estimation method via the simulation study, and the empirical study presents the advantages of the proposed MOGI model in portfolio allocation problems.

Data availability statement

The intraday data is provided by the Wharton Data Service (WRDS) (web link: <https://wrdswww.wharton.upenn.edu/>). Please note that the data sharing policy of WRDS restricts the redistribution of data.

References

- Admati, A. R. and Pfleiderer, P. (1988). A theory of intraday patterns: Volume and price variability. *The Review of Financial Studies*, 1(1):3–40.
- Aït-Sahalia, Y., Fan, J., and Xiu, D. (2010). High-frequency covariance estimates with noisy and asynchronous financial data. *Journal of the American Statistical Association*, 105(492):1504–1517.
- Aït-Sahalia, Y., Jacod, J., and Li, J. (2012). Testing for jumps in noisy high frequency data. *Journal of Econometrics*, 168(2):207–222.
- Aït-Sahalia, Y. and Xiu, D. (2016). Increased correlation among asset classes: Are volatility or jumps to blame, or both? *Journal of Econometrics*, 194(2):205–219.
- Aït-Sahalia, Y. and Xiu, D. (2017). Using principal component analysis to estimate a high dimensional factor model with high-frequency data. *Journal of Econometrics*, 201(2):384–399.
- Aït-Sahalia, Y. and Yu, J. (2009). High frequency market microstructure noise estimates and liquidity measures. *Annals of Applied Statistics*, 3(1):422–457.
- Andersen, T. G., Bollerslev, T., and Diebold, F. X. (2007). Roughing it up: Including jump components in the measurement, modeling, and forecasting of return volatility. *The review of economics and statistics*, 89(4):701–720.
- Andersen, T. G., Bollerslev, T., et al. (1997). Intraday periodicity and volatility persistence in financial markets. *Journal of Empirical Finance*, 4(2-3):115–158.
- Andersen, T. G., Thyrgaard, M., and Todorov, V. (2019). Time-varying periodicity in intraday volatility. Technical report.
- Barndorff-Nielsen, O. E., Hansen, P. R., Lunde, A., and Shephard, N. (2008). Designing realized kernels to measure the ex post variation of equity prices in the presence of noise. *Econometrica*, 76(6):1481–1536.

- Barndorff-Nielsen, O. E., Hansen, P. R., Lunde, A., and Shephard, N. (2011). Multivariate realised kernels: consistent positive semi-definite estimators of the covariation of equity prices with noise and non-synchronous trading. *Journal of Econometrics*, 162(2):149–169.
- Barndorff-Nielsen, O. E. and Shephard, N. (2006). Econometrics of testing for jumps in financial economics using bipower variation. *Journal of financial Econometrics*, 4(1):1–30.
- Bibinger, M., Hautsch, N., Malec, P., Reiß, M., et al. (2014). Estimating the quadratic covariation matrix from noisy observations: Local method of moments and efficiency. *The Annals of Statistics*, 42(4):1312–1346.
- Bollerslev, T. (1986). Generalized autoregressive conditional heteroskedasticity. *Journal of Econometrics*, 31(3):307–327.
- Bollerslev, T. (1990). Modelling the coherence in short-run nominal exchange rates: a multivariate generalized ARCH model. *The Review of Economics and Statistics*, pages 498–505.
- Bollerslev, T., Engle, R. F., and Wooldridge, J. M. (1988). A capital asset pricing model with time-varying covariances. *Journal of Political Economy*, 96(1):116–131.
- Candès, E. J., Li, X., Ma, Y., and Wright, J. (2011). Robust principal component analysis? *Journal of the ACM (JACM)*, 58(3):11.
- Christensen, K., Kinnebrock, S., and Podolskij, M. (2010). Pre-averaging estimators of the ex-post covariance matrix in noisy diffusion models with non-synchronous data. *Journal of Econometrics*, 159(1):116–133.
- Corsi, F., Pirino, D., and Reno, R. (2010). Threshold bipower variation and the impact of jumps on volatility forecasting. *Journal of Econometrics*, 159(2):276–288.
- Engle, R. (2002). Dynamic conditional correlation: A simple class of multivariate generalized autoregressive conditional heteroskedasticity models. *Journal of Business & Economic Statistics*, 20(3):339–350.

- Engle, R. F. (1982). Autoregressive conditional heteroscedasticity with estimates of the variance of united kingdom inflation. *Econometrica*, 50(4):987–1007.
- Engle, R. F. and Gallo, G. M. (2006). A multiple indicators model for volatility using intra-daily data. *Journal of Econometrics*, 131(1):3–27.
- Engle, R. F. and Kroner, K. F. (1995). Multivariate simultaneous generalized ARCH. *Econometric Theory*, 11(1):122–150.
- Fan, J., Furger, A., and Xiu, D. (2016). Incorporating global industrial classification standard into portfolio allocation: A simple factor-based large covariance matrix estimator with high frequency data. *Journal of Business & Economic Statistics*, 34:489–503.
- Fan, J. and Kim, D. (2018). Robust high-dimensional volatility matrix estimation for high-frequency factor model. *Journal of the American Statistical Association*, 113(523):1268–1283.
- Fan, J. and Kim, D. (2019). Structured volatility matrix estimation for non-synchronized high-frequency financial data. *Journal of Econometrics*, 209(1):61–78.
- Fan, J., Li, Y., and Yu, K. (2012). Vast volatility matrix estimation using high-frequency data for portfolio selection. *Journal of the American Statistical Association*, 107(497):412–428.
- Fan, J., Liao, Y., and Mincheva, M. (2013). Large covariance estimation by thresholding principal orthogonal complements. *Journal of the Royal Statistical Society: Series B (Statistical Methodology)*, 75(4):603–680.
- Fan, J., Wang, W., and Zhong, Y. (2018). An ℓ_∞ eigenvector perturbation bound and its application to robust covariance estimation. *Journal of Machine Learning Research*, 18(207):1–42.
- Fan, J. and Wang, Y. (2007). Multi-scale jump and volatility analysis for high-frequency financial data. *Journal of the American Statistical Association*, 102(480):1349–1362.

- Hansen, P. R., Huang, Z., and Shek, H. H. (2012). Realized GARCH: a joint model for returns and realized measures of volatility. *Journal of Applied Econometrics*, 27(6):877–906.
- Hong, H. and Wang, J. (2000). Trading and returns under periodic market closures. *The Journal of Finance*, 55(1):297–354.
- Jacod, J., Li, Y., Mykland, P. A., Podolskij, M., and Vetter, M. (2009). Microstructure noise in the continuous case: the pre-averaging approach. *Stochastic Processes and their Applications*, 119(7):2249–2276.
- Kim, D. and Fan, J. (2019). Factor GARCH-itô models for high-frequency data with application to large volatility matrix prediction. *Journal of Econometrics*, 208(2):395–417.
- Kim, D., Liu, Y., and Wang, Y. (2018). Large volatility matrix estimation with factor-based diffusion model for high-frequency financial data. *Bernoulli*, 24(4B):3657–3682.
- Kim, D., Song, X., and Wang, Y. (2020). Unified discrete-time factor stochastic volatility and continuous-time ito models for combining inference based on low-frequency and high-frequency. *arXiv preprint arXiv:2006.12039*.
- Kim, D. and Wang, Y. (2016). Unified discrete-time and continuous-time models and statistical inferences for merged low-frequency and high-frequency financial data. *Journal of Econometrics*, 194:220–230.
- Kim, D. and Wang, Y. (2021). Overnight garch-itô volatility models. *arXiv preprint arXiv:2102.13467*.
- Kim, D., Wang, Y., and Zou, J. (2016). Asymptotic theory for large volatility matrix estimation based on high-frequency financial data. *Stochastic Processes and their Applications*, 126:3527—3577.
- Kong, X.-B. (2017). On the number of common factors with high-frequency data. *Biometrika*, 104(2):397–410.

- Kong, X.-B. (2018). On the systematic and idiosyncratic volatility with large panel high-frequency data. *The Annals of Statistics*, 46(3):1077–1108.
- Kong, X.-B., Lin, J.-G., Liu, C., and Liu, G.-Y. (2021). Discrepancy between global and local principal component analysis on large-panel high-frequency data. *Journal of the American Statistical Association*, (just-accepted):1–32.
- Oh, M. and Kim, D. (2021). Effect of the us–china trade war on stock markets: A financial contagion perspective. *arXiv preprint arXiv:2111.09655*.
- Pelger, M. (2019). Large-dimensional factor modeling based on high-frequency observations. *Journal of Econometrics*, 208(1):23–42.
- Shephard, N. and Sheppard, K. (2010). Realising the future: forecasting with high-frequency-based volatility (heavy) models. *Journal of Applied Econometrics*, 25(2):197–231.
- Shin, M., Kim, D., and Fan, J. (2021). Adaptive robust large volatility matrix estimation based on high-frequency financial data. *Available at SSRN 3793394*.
- Song, X., Kim, D., Yuan, H., Cui, X., Lu, Z., Zhou, Y., and Wang, Y. (2021). Volatility analysis with realized garch-itô models. *Journal of Econometrics*, 222:393–410.
- Tao, M., Wang, Y., Yao, Q., and Zou, J. (2011). Large volatility matrix inference via combining low-frequency and high-frequency approaches. *Journal of the American Statistical Association*, 106(495):1025–1040.
- Tao, M., Wang, Y., Zhou, H. H., et al. (2013). Optimal sparse volatility matrix estimation for high-dimensional itô processes with measurement errors. *The Annals of Statistics*, 41(4):1816–1864.
- Wang, Y. and Zou, J. (2010). Vast volatility matrix estimation for high-frequency financial data. *The Annals of Statistics*, 38:943–978.
- Xiu, D. (2010). Quasi-maximum likelihood estimation of volatility with high frequency data. *Journal of Econometrics*, 159(1):235–250.

- Zhang, L. (2006). Efficient estimation of stochastic volatility using noisy observations: A multi-scale approach. *Bernoulli*, 12(6):1019–1043.
- Zhang, L. (2011). Estimating covariation: Epps effect, microstructure noise. *Journal of Econometrics*, 160(1):33–47.
- Zhang, L., Mykland, P. A., and Aït-Sahalia, Y. (2005). A tale of two time scales: Determining integrated volatility with noisy high-frequency data. *Journal of the American Statistical Association*, 100(472):1394–1411.